5th Quarterly Progress Report
October 1 to December 31, 2001

Neural Prosthesis Program Contract N01-DC-0-2108

Protective Effects of Patterned Electrical Stimulation on the Deafened Auditory System

Submitted by:

Russell L. Snyder
Julie A. Bierer
University of California at San Francisco
and
John C. Middlebrooks
Kresge Hearing Research Institute, Neuroscience Program, University of Michigan, Ann Arbor, MI.

Epstein Hearing Research Laboratories
Department of Otolaryngology, Room U490
University of California, San Francisco
San Francisco, Ca 94143-0526

ABSTRACT

In this Quarterly Progress Report we describe preliminary studies using newly-developed multichannel recording methods to assess the spread and intensity of CNS activation in response to acoustic and electrical stimulation of the cochlea. In brief, animals were anesthetized and a 16-channel silicon recording probe was inserted into the inferior colliculus (IC) on the left side. Accurate placement, i.e. spanning the normal frequency distribution of the IC, was assured by inserting the probe until the tonotopic response regions recorded along the length of the probe reflected the appropriate IC locations for acoustic tones delivered to the contralateral ear. That is, when the best frequencies for the 16 sites arrayed along the probe ranged sequentially from 2-20 kHz. Following this calibration process, the recording probe was fixed in place, the best frequency (BF) of each recording site was determined and the animal was acutely deafened with an injection of neomycin sulfate into the scala tympani. Once the probe was fixed in place the subject could then be moved to permit full surgical access to the scala tympani allowing either the testing of model scala tympani stimulating arrays or the individual placement of stimulating contacts on specific structures within the cochlea to compare performance.

The spread of cochlear activation by an electrical stimulus depends on the configuration of the stimulating electrodes relative to cochlear structures. In this study we stimulated the guinea pig cochlea acoustically and then with three types of intracochlear electrodes. These included a modified 6-channel Nucleus banded array (Cochlear Corp., Englewood, CO) and a modified 4 channel UCSF off-radial array, both similar to current clinical devices (Rebscher et al., '99). In addition, we used a pair of independently placed platinum/iridium wires terminated as 250 μm balls, which were placed with visual control on identified cochlear structures. The intracochlear spread of activation was estimated by recording single and multi-unit neuronal activity along the tonotopic axis of the central nucleus of the inferior colliculus (ICC). Electrical stimuli consisting of single biphasic electrical pulses were presented with each electrode type.

Monopolar stimulation (an intracochlear active electrode vs. an extracochlear return) with all electrode types produced very broad excitation in the ICC. Bipolar stimulation with the Nucleus banded electrode produced activation that was somewhat less broad. Nucleus-tripolar and UCSF-off-radial bipolar configurations produced more restricted ICC activation. Bipolar stimulation with the visually placed balls in a radial configuration produced the most restricted activation, which was comparable to that of a pure tone. When the distance between *radially* oriented balls was varied, it had little effect on the spread of ICC activation, although there were systematic differences in threshold. When the two bipolar electrodes were longitudinally oriented along the cochlear spiral produced broader ICC activation, wider separation between longitudinal pairs led to broader ICC activation.

INTRODUCTION

Cochlear implants (CIs) are very successful prosthetic devices and have become the 'standard-of-care' for severely to profoundly deaf adults and children. Worldwide, approximately forty five thousand individuals, many of them profoundly deaf, have received cochlear implants. Many of these receive sufficient benefit from one of the several commercially available CI systems that 83% of them talk on the telephone on a regular basis and 29% carry on interactive telephone conversations (Mawman et al, 2000).

In the development of these devices, arguably the two most important advances have been the introduction of multi-channel speech processors and of multi-contact intracochlear stimulating electrodes. Multi-channel processors break the incoming acoustic signal into a series of frequency bands. Each processed band is delivered to a designated contact (or pair of contacts) in the multi-contact, intracochlear electrode. In an optimal implant, each contact would selectively activate *a restricted and appropriate* sector of the auditory nerve array. Activation selectivity is important, since selective auditory nerve activation is the *sine qua non* of multi-channel intracochlear stimulation. If all contacts activate the same fiber population, multi-channel stimulation is impossible. However, the selectivity of any particular CI design has been difficult to document and the factors governing electrode selectivity are poorly understood. Numerous psychophysical, physiological and computer modeling studies have attempted to estimate the effects of different electrode configurations on the spread of intracochlear activation, channel interaction and activation selectively, but there is little agreement among these studies.

Comparisons of results across these studies to determine the factors governing stimulus selectivity are difficult. In human studies to date, each study employed a single, and unique stimulation paradigm, different intracochlear electrode types and different stimulus waveforms. There are now at least five different intracochlear electrode designs for human implantation, three different stimulation modes (monopolar, bipolar and common ground) and several different processing strategies (e.g., CIS, SPEAK, SAS, etc.). Animal studies have used at least three electrode designs including modified Nucleus™ electrodes (a series of longitudinally arrayed bands on a cylindrical silicone carrier), modified UCSF or Clarion™ electrodes (a series of ball electrodes on a tapered silicone carrier), and simple wire-and-ball electrodes (independently placed balls with no silicone carrier). The studies have used different electrode orientations (longitudinal, radial or off-radial), and they have used different stimulation configurations (monopolar, bipolar or tripolar). In addition, these studies employ subjects in which the mode and duration of deafness are highly variable, which leads to variability in both the distribution and overall number of surviving auditory nerve fibers (Leake et al, 1991; Fayad et al 1991; Nadol et al, 1989; Nadol, 1997). Thus, the reported results are highly variable both within and among the studies. *Some studies report results that suggest highly restricted evoked-activity patterns along the cochlear spiral and its central connections, which are comparable to patterns evoked by acoustic stimuli in human (*Eddington et al, '78, Tong et al, '82; Shannon, '83, Tong and Clark, '85, Townshend et al, '87; Nelson et al, '95; Busby et al, '94) and animal studies (*Snyder et al., 1990; Ryan et al., 1990; Brown et al., 1992). Others report very broad and/or idiosyncratic activation patterns (Kral et al., 1998;Shepherd et al., 1999; Raggio and Schreiner, 1999; Arenberg-Bierer and Middlebrooks, 2001) or examples of both observations depending upon the stimulation conditions of each trial (Rebscher et al., 2001; Van den Honert, et al., 1987).*

In this study, we have tried to eliminate some of these compounding variables and to examine some of the factors controlling activation selectivity by studying these factors in a single animal using a

single recording electrode. We have chosen to record the responses of neurons in the central nucleus of inferior colliculus (ICC) of the guinea pig both before and after acute deafening. We have used single tine, 16-channel, recording silicon-microprobes to record these responses. The probes were inserted along a standardized trajectory such that the recording contacts were arrayed across the tonotopic organization of the guinea pig ICC. These electrodes were fixed in place and the responses to acoustic tones were recorded. These acoustically evoked responses allowed us to determine the characteristic frequencies (CFs) of the neurons surrounding each recording site. Once the probe had been 'calibrated' using acoustic tones, the animal could be deafened and the responses to various intracochlear electrical stimuli and one or more intracochlear electrodes could be evaluated. Using this method, we directly and quantitatively compared the excitation patterns produced by various types of intracochlear electrical stimulation.

METHODS

Anesthesia and surgery:

Data were collected from 13 healthy adult pigmented guinea pigs (500–900 g). Twelve of these animals had normal hearing. One animal was deafened with an intracochlear injection of neomycin sulfate 2 weeks prior to the experiment. Animals were initially sedated with a subcutaneous injection of a 3:2 mixture of ketamine hydrochloride (100 mg/ml) and xylazine (100 mg/ml). Additional intramuscular injections of a 4:1 mixture of ketamine/xylazine were given as needed to maintain an areflexive state. Heart rate, respiratory rate and body temperature were monitored continuously. Core body temperature was maintained at 38°C with a thermostatically controlled heating pad. A tracheal cannula was inserted to insure an unostructed airway. A dorsal midline incision was made in the scalp to expose the dorsal surface of the skull. The head was fixed in place by attaching a phenolic rod, which was fixed to the skull anterior to the bregma using small self-tapping screws and dental acrylic. The phenolic rod was held by a clamp connected to a vertical post that screwed into a large horizontal metal base-plate. The temporalis muscle was reflected, and a 5 mm opening was made in the right parietal bone just dorsal to the parietal/temporal suture and just rostral to the tentorium. The dura was incised and reflected to expose the lateral and posterior occipital cortex. This cortex was aspirated to visualize the dorsal and lateral surface of the IC.

Once the IC was visualized and all bleeding stopped, a silicon-substrate, thin-film, multi-channel-recording probe (Center for Neural Communication Technology, Ann Arbor, MI) (Drake et al. 1988; Najafi et al. 1985) was inserted manually using a micromanipulator (Narishige) into the center of the IC. The probe was rigidly mounted on a custom-built pre-amplifier that was held by the micromanipulator. The probe was inserted into the IC on a dorsolateral to ventromedial trajectory at a 45º angle off the parasaggital plane in the coronal plane. Using this trajectory, the probe traversed the central nucleus of the IC at a right angle to its iso-frequency laminae (Snyder et al., 1990.1991, 2001). Each probe had 16 recording sites along a single shank distributed at 100-µm intervals (center to center). The shank was 15 µm thick and 100 µm wide at the most proximal site and tapered to 15 µm at the most distal point. The impedances at each site were 1.5–4 MΩ. In the guinea pig, the 1.5 mm distance from the most distal to the most proximal recording site allowed simultaneous recording of responses from neurons sensitive to frequencies spanning approximately 4.5 octaves . The probes were inserted manually until the most distal site recorded activity from neurons with a characteristic frequency (CF) of approximately 18 kHz. Once this location had been reached, the cortical deficit was filled with warm 2% agar dissolved in Ringer's solution. When the agar had solidified, the agar and the surrounding parietal and temporal bones were covered with a thick layer of dental acrylic sealing the bony deficit and

fixing the probe in place. After the probe had been fixed in place, acoustic responses from all 16 electrodes were recorded from these normal hearing animals. The acoustic responses were evoked by contralateral tones (see below) at three levels separated by 20 dB (usually 20, 40 and 60 dB SPL). Tone frequencies were separated by 1/6 of an octave and ranged from 1 to 20 kHz.Once these preliminary acoustic recordings had been made and the probe was fixed in place, the probe was detached from its pre-amplifier and the animals were rotated 180 degrees along and around their rostrocaudal axis (head-to-tail and right-ear-up to right-ear-down). This allowed access to the left (contralateral) cochlea after insertion of the probes into the right IC. After rotation, a second series of acoustic responses were recorded. In all cases, post-rotation responses were not detectibly different from the pre-rotation responses. These acoustic recording allowed both a relative depth and a CF to be assigned to each probe recording site, effectively calibrating the sites to a series of cochlear locations. After this second series of acoustic recordings, the left cochlear bulla was exposed and opened, so that the round window could be visualized. A silver wire was placed in the round window niche and fixed to the overlying temporal bone with cyanoacrylate glue. This silver wire served as the active electrode to record the click evoked compound action potential (CAP) from the auditory nerve. Two electrodes in the scalp served as the reference and ground electrodes. The CAP threshold was determined and then the animals were deafened by injecting a 10% solution of the cochleotoxic drug, neomycin sulfate, into the cochlea through a small slit in the round window membrane. Infusion of neomycin was continued while recording click-evoked responses until the CAP threshold exceeded the output of our system.

After the animals were deafened, a second silver electrode was placed on the oval window and fixed to the surrounding temporal bone with cyanoacrylate glue. A cochleostomy was made in the lateral wall of the cochlea at the junction of the 'hook' and first turn of the cochlea. A modified Nucleus banded electrode, which consisted of the 6 most distal bands of a human cochlear implant, was inserted into the scala tympani. After insertion, responses were recorded after activation of different intracochlear electrode contacts in different configurations (monopolar, bipolar or tripolar). When these responses had been recorded, the Nucleus electrode was removed. The cochleostomy was enlarged and a modified UCSF electrode was inserted. This electrode consisted of two off-radial pairs (an apical and a basal pair) of ball contacts, 250 µm in diameter, in a silastic carrier (Rebscher et al., 2001). The contacts of the off-radial pairs were separated by 1 mm and the pairs were separated by 2 mm. Responses to activation of this UCSF electrode were then recorded using several stimulation configurations (monopolar or bipolar). After recording these responses, the UCSF electrode was removed and the cochleostomy was further enlarged so that two insulated platinum/iridium wires ending in 250 µm balls could be placed visually within the basal scala tympani using a dual micromanipulator (Narishige). These balled contacts were placed at different locations within the basal turn and the responses evoked by their activation were recorded across the 16 channels of the fixed probe. All procedures were conducted in accordance with the policies of the University of Michigan's University Committee on Use and Care of Animals.

Stimulus generation and calibration:

Acoustic signals: Experiments were controlled by an Intel-based personal computer. Acoustic stimuli were synthesized digitally using equipment from Tucker-Davis Technologies (TDT) (Gainsville, Florida). The sample rate for audio output was 100 kHz with 16-bit resolution. Experiments were conducted in a sound-attenuating chamber. Sound stimuli were presented monaurally to the ear contralateral to the studied inferior colliculus. A headphone enclosed in a small case was connected to a sound-delivery tube inserted into the external auditory meatus near the tympanic membrane and sealed in place using dental acrylic. The headphone was calibrated using a 1/8-in. condenser microphone (Büel

& Kjær) and a 0.3-cc coupler. The resulting calibration table was used for online correction of the headphone response. Tone and noise bursts were 80–100 ms in duration. Tones were ramped on and off with 5-ms rise/fall times, and noise bursts had 0.5-ms rise/fall times. Broadband Gaussian noise bursts had a passband of 1–30 kHz with abrupt cutoffs. Sound levels of tones and noise bursts were equated for root-mean-squared power. The sets of center frequencies, bandwidths, and levels varied from animal to animal. Stimulus center frequencies ranged from 1–20 kHz in either 1/3- or 1/6-octave steps. Levels ranged from 0 to as high as 90 dB sound pressure level (SPL) in 10-dB steps.

Multi-channel recording and spike sorting:

The multi-channel probe permitted simultaneous recording of spike activity from all sites. Signals from the recording probe were amplified with a custom 16-channel amplifier, digitized at a 25-kHz rate, sharply low-pass filtered below 6 kHz, re-sampled at a 12.5-kHz sample rate, and then stored on the computer hard disk. Unit activity was isolated from the digitized responses off-line using custom spike-sorting software (Furukawa et al. 2000). Spike times were stored at a resolution of 20-μs for further analysis. Well-isolated single units were recorded as well as multiunit clusters consisting of a small number of unresolved units. However, since in all cases the responses were indistinguishable at the levels of analysis used in this study, they were treated identically. Recordings at particular sites were excluded from further analysis if units did not respond to any stimulus with an average of at least 1 spike/trial or if the mean spike count changed by more than a factor of 2 over the recording period.

Data analysis:

Spike counts were normalized at each recording site according to the 95th percentile of the average spike counts computed within one wideband stimulus type (a wide band noise of acoustic stimulation and electrical activation with bipolar electrodes placed on the round window and oval window). By normalizing in this manner, we emphasized stimulus-driven changes in activity rather than differences in absolute spike counts across channels. The results include data from individual recording sites as well as the distribution of activity across multiple recording sites. For individual recording sites, the lowest level that elicited a stimulus-locked response was defined as threshold. The *best frequency* (BF) was defined as the frequency that gave the strongest response at 10 dB above threshold. The *best location* (BL) was defined as the recording site that produced driven activity at threshold. The *tuning bandwidth* at any particular sound level was taken as the width of the spike-count-versus-frequency function at the interpolated half-maximal spike count for that stimulus sound level. In some cases, the spike-count-versus-frequency function did not cross the half-maximal spike count at either the high end or the low end of the tested frequency range. In these cases, the 50% frequency cutoff was estimated to be halfway between the 75% cutoff frequency and the next extrapolated frequency, usually 1/3 octave beyond the tested range. If the spike-count-versus-frequency function did not cross at least the 75% cutoff frequency on both sides, then the tuning bandwidth was not computed for that site. The tuning bandwidth was calculated for pure tones and wide band noise at levels 10, 20, and 30 dB above each unit's threshold. The temporal distribution of activity across all recording sites was referred to as an IC *spatiotemporal image* (STI). The *centroid* of the image was defined as the spike-count-weighted center of mass calculated for the sites at which the firing rate was at least half the maximum normalized spike count of the distribution.

RESULTS

Neural Activity:

Figure 1 illustrates four oscilloscope traces, 45 ms in duration, which represent neural activity recorded at two sites (#9 top pair and #12 bottom pair) on one probe in the ICC of one guinea pig. The top recording in each pair was recorded early in the experiment (trial #122) and the bottom recording in the pair was recorded late in the experiment (trial #14696) approximately 12 hours apart. The activity observed in all four recordings was evoked by an intracochlear electrical pulse, which was presented at the beginning of each trace. Although there is no electrical artifact visible in these recordings, electrical artifacts were often observed, especially at the highest current levels. However, this artifact was always confined to the first 1-3 ms of the recordings and was eliminated as a source of contamination in our data analysis by delaying the counting of all spikes until after the artifact had disappeared. The circles above the spike waveforms are indications that these waveforms were recognized as spikes by our spike-sorting algorithm. By comparing the activity recorded at site #9 with that recorded at site #12 one can see that the quality of recordings varied within an animal and among the sites from a single probe. The recordings at site #9 are representative of sites at which there is relatively good isolation of the activity from a single neuron. The recordings at site #12 are representative of sites at which there was relatively poor isolation among neurons. Recordings such as those at site #12 are termed multiunit recordings, although there are clear single units discernable. By comparing the recordings made during stimulus trial# 122 with those made during trial# 14626 at each site (top vs. bottom of each pair), one sees that the quality of the recordings made at any given site changed very little over the 12-18 hr experimental interval. In addition to recordings such as these, little or no neural activity could be recorded at some sites. However, these silent sites were unusual. We estimate that they represented 5% of the sites that we examined. In most cases, all probe sites recorded some neural activity and that activity fell between the extremes illustrated in Figure 1.

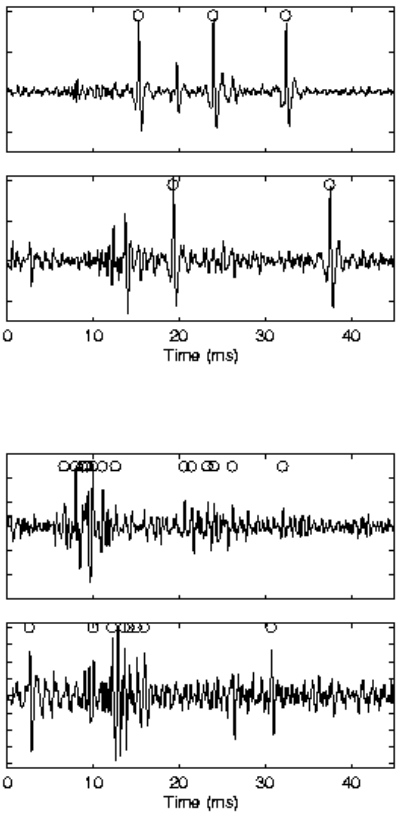

Figure 1. Raw traces from GP200026. **UPPER** two rows show raw recordings from the recording site 0.8 mms from the most superficial site. **LOWER** two rows show raw recordings from the recording site 1.1 mm from the most superficial site. The trial from which the data were obtained is indicated to the right of each panel. The top panel of each pair of panels was obtained early within an experiment while the lower of each pair of panels was obtained several hours later in the same experiment. The example shown in the top two panels shows an isolated single unit while the lower example shows a multi-unit cluster. In most cases, a multi-unit cluster was observed.

Acoustic Stimulation:

At the beginning of each experiment, a matrix of acoustic tones, which varied across a wide range of frequencies and intensities, were presented to the cochlea contralateral to the recording site in the IC. Quantifying the responses evoked by these tones, allowed us to construct frequency response areas (RAs) at each site. From these RAs, a best frequency (BF) can be determined for each site. Four representative RAs are illustrated in Figure 2. These examples were recorded at 4 sites along one probe in the ICC of one animal. Their excitatory regions have the 'V' shape that is typical for ICC neurons under Nembutal anesthesia. They are arranged sequentially according to their ICC depth with the RA from the most superficial site (#1) on the left and that from at deepest site (#13) on the right. The estimated BF at these sites shifts systematically from 4.2 kHz at the most superficial site to 17 kHz at the deepest site.

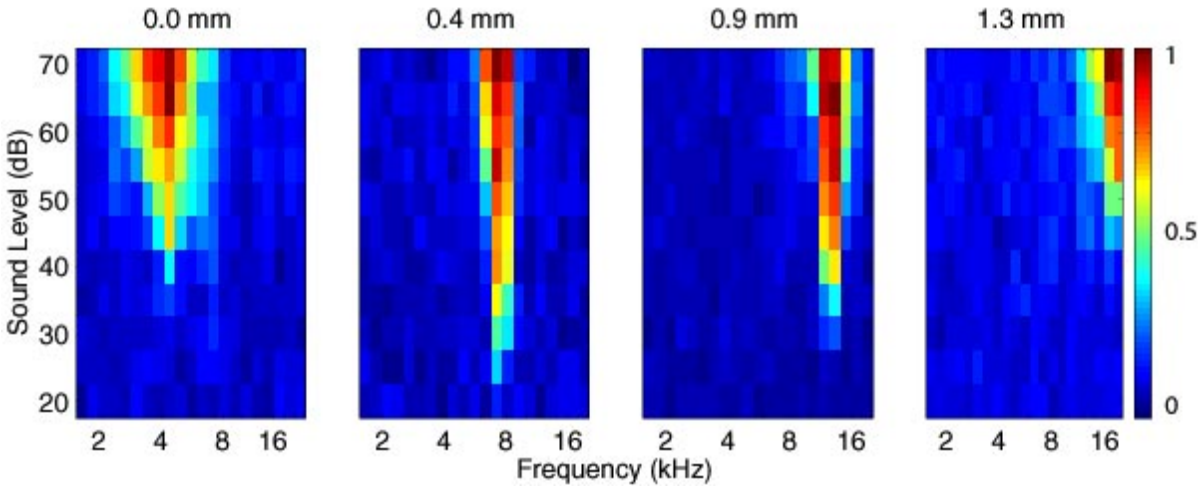

Figure 2. Response areas (RAs) recorded simultaneously at four locations (four sites) along a silicon probe in the ICC of a guinea pig (GP200016). Each RA is constructed by counting the number of spikes evoked by a matrix of 20 tones between 2 and 18 kHz presented at 11 levels between 20 and 70 dB SPL. Normalized spike counts are color coded according to the scale at the far right.

Using the same responses to acoustic stimulation, iso-intensity frequency maps (IFM's) can be constructed of responses to 20 tones, which range in frequencies from 2 to 16 kHz at a single intensity. Four representative examples of such IFM's are illustrated in Figure 3. The 4 IFM's are simultaneous 40 ms recordings of responses to 20 tones at four sites along one probe in the ICC of one animal. As in figure 2, the IFM's are arranged sequentially with the IFM from the most superficial site (#3) on the left and that from the deepest site (#15) on the right. These frequency maps illustrate the magnitude and temporal properties of the responses at each site to the 20 tones. Each horizontal row of facets in an IFM represents of the responses to one tone and is equivalent to a post-stimulus time histogram (PSTH) in which the magnitude of the response is represented in pseudocolor. By scanning down the frequencies and summing the number of discharges evoked by each tone, the BF at each site can be estimated. Again, as in Figure 2, there is a systematic shift in BF with depth in the ICC.

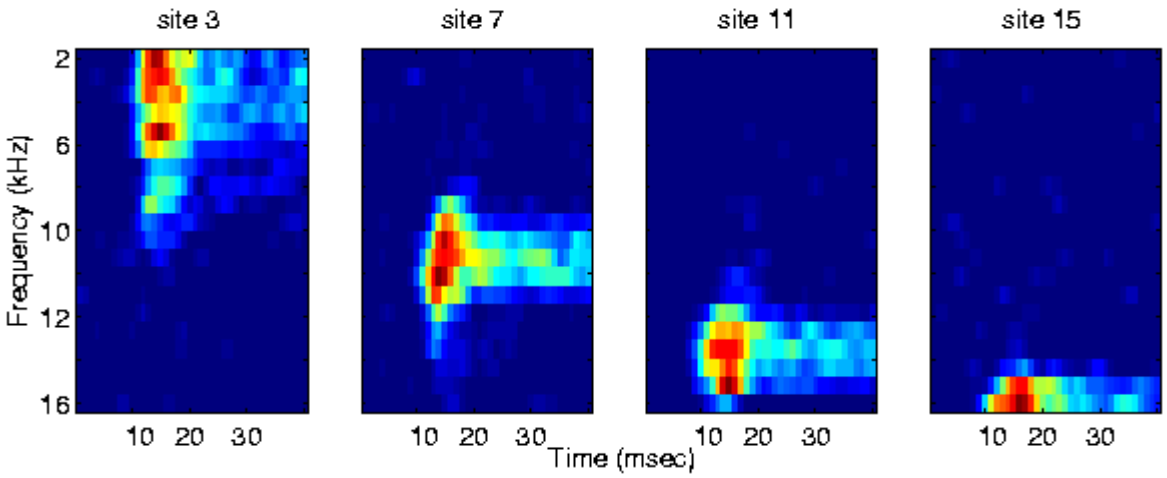

Figure 3. Iso-Intensity response maps recorded simultaneously at four locations along a single probe for tones presented at intensities 20 dB above their threshold. Tone bursts were 40 ms in duration and 2 ms rise/fall times. Tone onsets began at 0 ms. Data from GP200025.

The frequency gradient (FG) along each probe can be estimated by plotting the BF at each site as a function of ICC depth (site location). If the tonotopic gradient across the ICC of all guinea pigs were identical, and if the probes were inserted to the same depth along identical trajectories, then the frequency gradients observed along the probes from different animals would be identical. Figure 4 illustrates the frequency gradients for probes inserted in 9 guinea pigs. Although two of these gradients have slightly different slopes, 7 of these gradients show remarkable similarity. Previous studies in cats using tungsten microelectrode recording at fixed penetration intervals have shown similar uniformity among individuals (Schreiner and Langner, 1988; Snyder et al., 1990; 2000; 2001; Fuzessery, 1994).

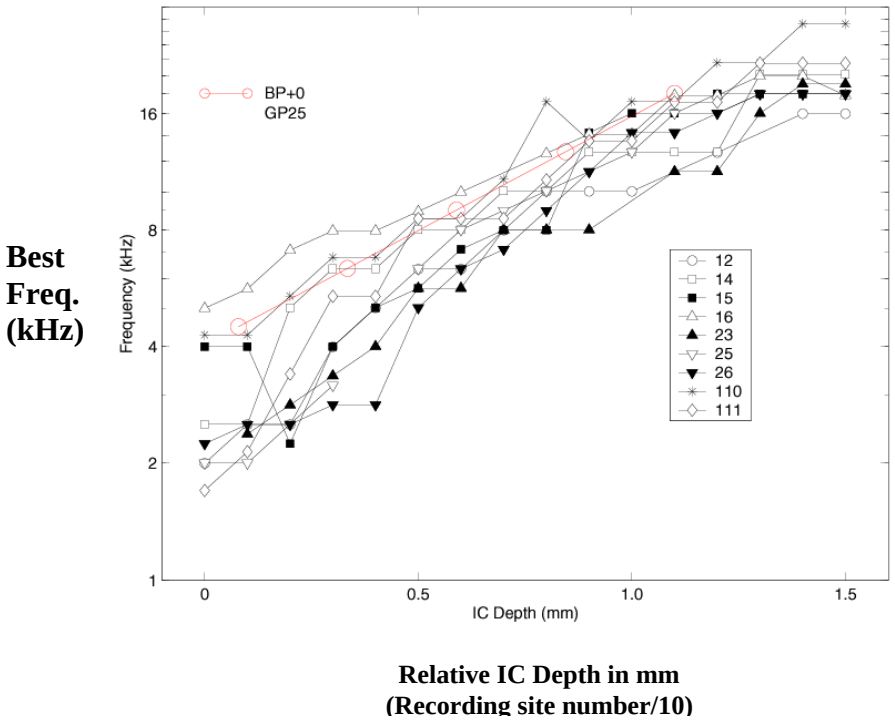

Figure 4. Frequency gradients (black lines) recorded from single probes in 9 animals. Abscissa is probe location or relative depth in the IC. Ordinant is best frequency in kHz.

Although the response measures illustrated so far (RA's, IIM's, FG's) are among the standard measures used to characterize acoustically evoked neural responses in the IC, analogous measures are difficult to obtain for electrical stimulation. They require stimulation that is restricted to several different regions of the basilar partition at different intensities, while recording from a single neuron or cluster of neurons. However, Figure 5illustrates one of several response measures for which analogous measurements can be obtained. This measure, which we call an IC spatiotemporal image (STI), plots response magnitude against IC depth (relative site location) and post-stimulus time. An IC STI can be constructed using either acoustic or electrical stimuli. Figure 5 (top row) illustrates images evoked by 4 single tones. Each STI is evoked by a single tone at a single intensity. The stimulus frequencies range from 2 kHz (far left) to 16 kHz (far right) in roughly one octave steps. Each tone is presented at 20 dB above its threshold, the lowest level at which it evoked a response at any site. The frequencies of the tones are indicated above each image. The probe site at which each tone evokes the largest and/or the most sustained response with the shortest latency is called the 'best location' or BL for that tone. As expected from the tonotopic organization of the ICC, BLs shift ventrally with higher tone frequency. At each frequency, the responses at locations above and below BL occur with a longer latency, have a smaller response magnitude and tend to produce a more transient or onset-only response. It is interesting to note that often the largest transient response is not produced at BL, but often occurs at locations either above (see 16 kHz, 20 dB response) or below (see 7.1 kHz, 30 dB response) it.

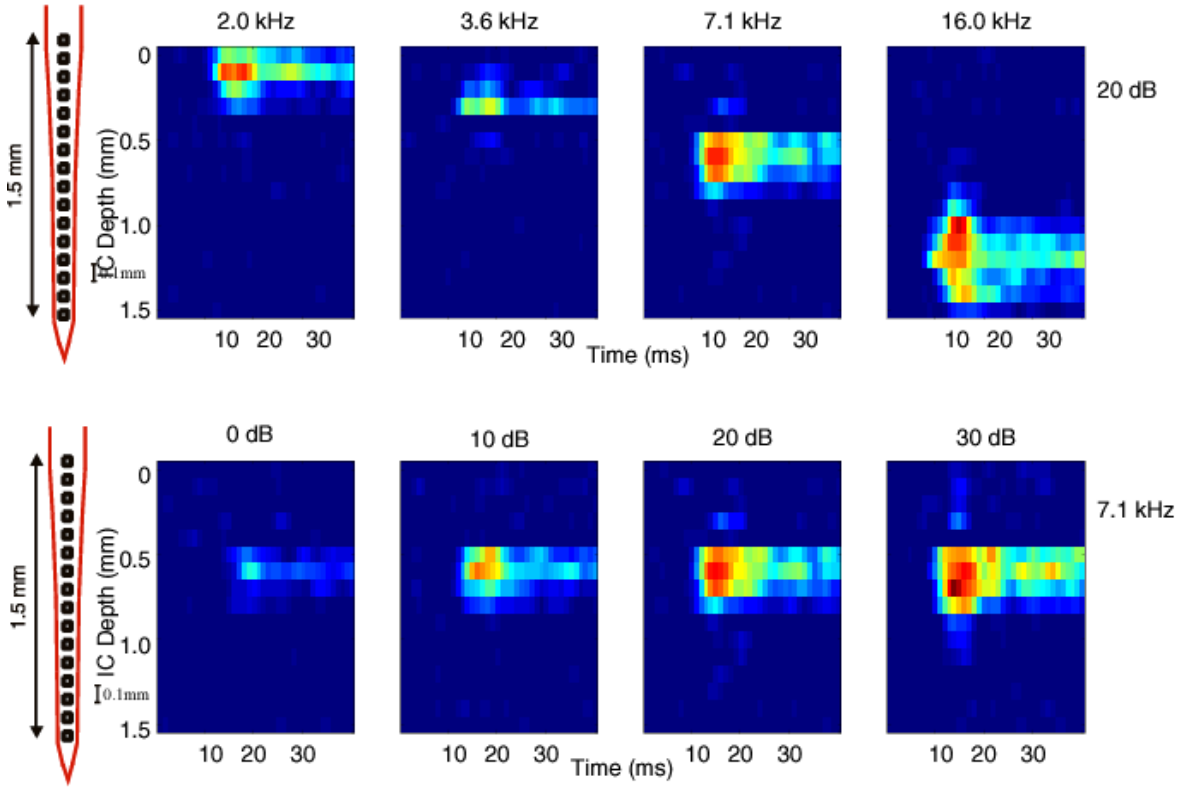

Figure 5: UPPER ROW shows spatiotemporal images (STIs) of tones at 2, 3.6, 7.1 and 16 kHz. In each image, the vertical dimension shows ICC depth (i.e., distance along the recording probe), the horizontal dimension shows post-stimulus time, and the colors represent normalized spike rates. The regions of excitation within these ICC images shifted progressively deeper in the ICC as stimulus frequencies increased. **LOWER ROW** shows STIs for a 7.1 kHz tone at four intensities relative to threshold (0, 10, 20 and 30 dB). The axes are as represented in the images in the upper row. The region of excitation in these images spreads across the electrode array as stimulus intensity increases.

The 4 STIs along the lower row of Figure 5 illustrate the spread of activation by stimulation at increasing intensities using a single frequency. They show responses evoked by a single tone (7.1 kHz) presented at 4 intensities (0, 10, 20 and 30 dB re threshold). At intensities near threshold, responses are restricted to 1- 3 recording sites (0.5-0.7 mm in Fig. 5). At higher stimulus levels, the response spreads to adjacent recording sites both above and below BL. Typically, this spread is greatest during the onset (the first 5-10 ms) period of the response, whereas the sustained or steady-state responses remain more restricted usually to the few locations activated at threshold. This restricted steady-state activation occurs even at high levels. In addition to the spread of excitation with increasing intensity, there is also a decrease in latency. As stimulus intensity increases, latencies decrease, but they decrease most at BL. In Figure 5, the shift in latency is 6 ms at BL (0.6mm) and only 2 ms at locations 0.3 mm above and below BL. This differential effect of intensity on latency at different sites contributes to the chevron-shaped activity pattern seen in the onset response. This chevron pattern combined with a sustained response, which is restricted to sites surrounding BL, produces an arrow-like activity pattern over space and time in these images.

Each STI presented in Figure 5 illustrates the spread of excitation across time and space in the ICC of one stimulus at a single intensity. Together they demonstrate that stimulus intensity dramatically affects latency and the spread of excitation. These effects at several intensities can be summarized by constructing spatial tuning curves (STCs). The STCs in Figure 6 summarize the spread of excitation across the depth of the ICC as a function of stimulus intensity. Each curve consists of a series of iso-rate contours plotted as a function of depth (site location) and stimulus intensity. As described in the methods, the rates are the normalized relative to the maximum response evoked by any stimulus at each site. In the four STCs in Figure 6, there are four iso-rate contours, which represent responses from 0 to 90% of the maximum response at each location. The left two panels in Figure 6 illustrate an STC recorded in response to broadband noise. It demonstrates a broad activity pattern. At low levels, the contours are vertical stripes showing little site selectivity, i.e., approximately the same rate response at all locations. At higher levels, the contours are irregular patches with maximum rate responses at idiosyncratic locations within the depth/intsensity matrix. The next three panels in Figures 6 illustrate STCs recorded in response to tones (5, 11 and 22kHz, respectively). In these tone STCs, the contours are a series of nested ‘V’s indicating significant site selectivity at all stimulus intensities. For example, a 5kHz tone (Fig. 6b) activates only site 2 at 35dB and activates only the four most superficial sites at the highest intensities. Thus, site 2 is the best location (BL) for 5kHz. In figure 6c, a 10kHz tone activates a broader range of locations, but it activates only site # 6 (the BL) at the lowest level and produces the highest rates at this site at all intensities.

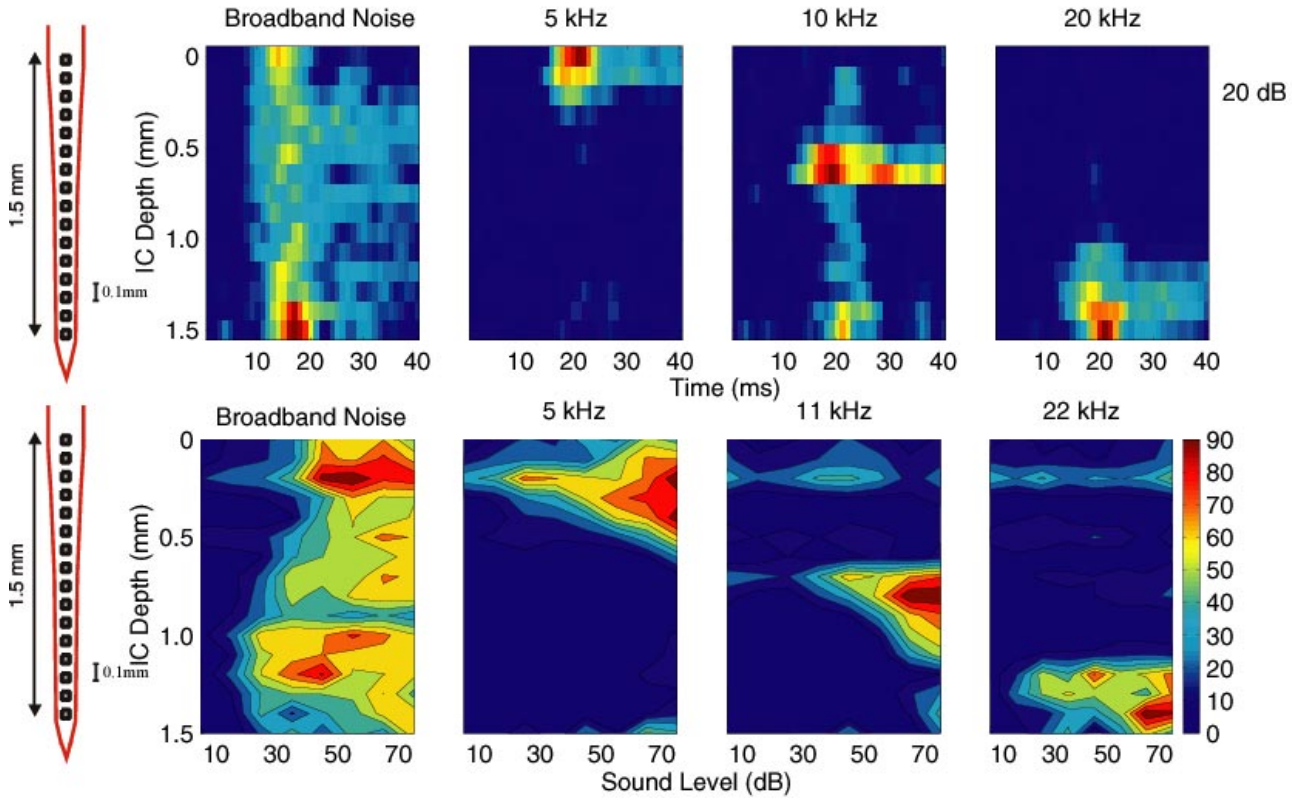

Figure 6: UPPER ROW shows STIs evoked by Gaussian noise and tones bursts at 5, 10, and 20 kHz. In each image, the vertical dimension shows ICC depth (i.e., distance along the recording probe), the horizontal dimension shows post-stimulus time, and the colors represent normalized spike rates along the pseudocolor scale shown along the lower right. The Gaussian noise bursts evoke excitation at all sites along the recording probe, whereas tones evoke excitation that is restricted to specific recording sites. The regions of excitation evoked by the tones shifted progressively deeper in the ICC as stimulus frequencies increased. **LOWER ROW** shows spatial tuning curve (STCs) from the same animal. The axes represent ICC depth (ordinate) and sound level (abscissa), and the contours represent stimulus values that produced normalized spike rates along the pseudocolor scale shown along the lower right. In each panel, activity was spatially restricted at near-threshold levels. At higher stimulus levels activity spread along the tonotopic axis. Again, a tonotopic organization is evident. Percentage of normalized spike rate is shown on the color scale on the right.

The spatiotemporal images (STIs) and spatial tuning curves (STCs), which are analogous to those evoked by acoustic stimuli, can be constructed for responses evoked by ICES. In the present study, we have recorded STIs and STCs to acoustic **and** ICES in each animal. We have used the acoustic responses to calibrate our recording electrodes, i.e., to specify the BF of each electrode and the BL of a series of acoustic frequencies. We then deafened these animals and recorded the responses evoked by ICES applied using three types of intracochlear electrodes: visually placed bipolar electrodes, a modified version of the banded Nucleus 22 electrode (it has only 6 bands) and a four contact version of the UCSF electrode. The STIs and STCs evoked by these three intracochlear electrodes will be considered in order.

Intracochlear Electrical Stimulation:

Visually Placed (VP) Electrodes: An image of a visually placed electrode pair is shown in Figure 7. In this figure, the lateral wall of the bulla has been removed exposing the lateral wall of the cochlea. The basal end of the cochlea is to the left and the apical end is to the right. The four turns (I, II, III and IV) of the cochlea are labeled. The lateral wall of the basal end of the basal turn has been removed enlarging the round window (dotted oval) and exposing the basilar membrane (arrows) of the 'hook' region and basal end of the 1st cochlear turn. The visually placed electrodes are located on the osseous spiral lamina (osl) in a radial configuration with one electrode (a) placed on the habenula and another (b) placed on top of the spiral ganglion. Since these electrodes can be moved individually, their orientation relative to intracochlear structures and the separation between them can be varied systematically.

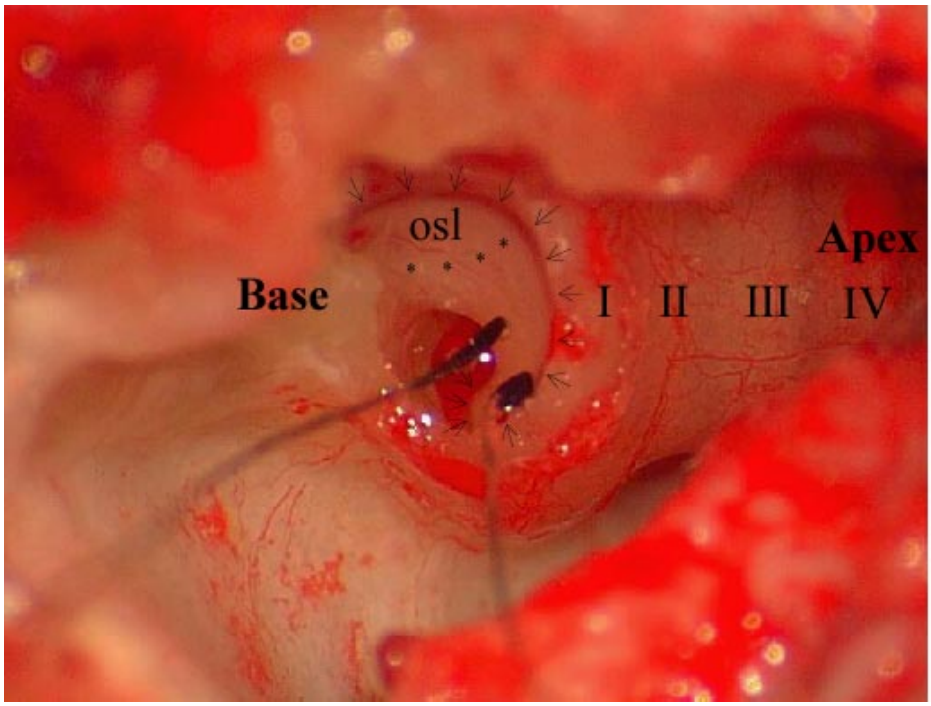

Figure 7. Image of two visually placed, radial bipolar electrodes. The lateral wall of the bulla and cochlear basal turn have been removed so that the osseous spiral lamina (osl) can be seen in the hook and initial basal turn regions of the cochlea The lateral edge of the round window is indicated by the asterisks. The peripheral edge of the basilar membrane is indicated by the arrows. The four turns of the guinea pig cochlea are indicated by the roman numerals (I-IV).

The effects of electrode placement in one animal are illustrated in Figure 8. This figure shows the STCs evoked by electrode placements on the osseous spiral lamina at successively more basal (higher frequency) locations within the cochlea: the 2nd turn (Fig. 8A), the 1st turn (Fig. 8B) and the middle of hook region (Fig. 8c) of the cochlea. These placements result in activity patterns that have their best locations (BLs) and regions of maximum activation at successively more ventral (higher frequency) locations along the probe. Stimulation of the 2nd turn produces activation, which has a BL and maximum response at 0.4 mm along the recording electrode array. Stimulation of the 1st turn produces activation, which has a BL and maximum response centered at 1.0 mm and stimulation of the hook

region produces activation, which has a BL and maximum response centered at 1.4 mm). These locations correspond to BLs of approximately 4, 10 and 18 kHz respectively. Thus, shifting the intracochlear location of a radially oriented VP electrode pair along the cochlear spiral produces spatially restricted activation of the appropriate region of the tonotopically organized ICC.

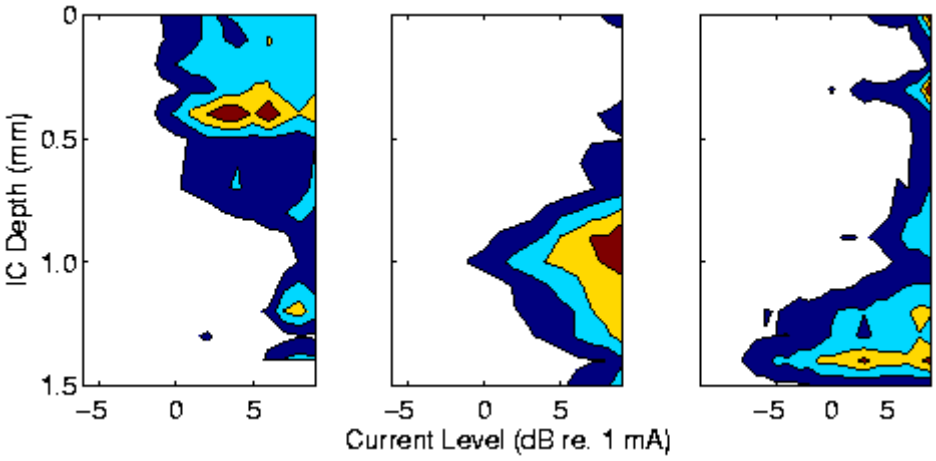

Figure 8. Spatial tuning curves illustrating the spatial distribution of activity evoked by electrical pulses delivered via visually placed (VP) electrodes. All stimuli were single biphasic pulses 40 µs/phase. **A.** VP electrodes in the 2nd turn. **B.** VP electrodes in the apical 1st turn. **C.** VP electrodes in the basal 1st turn. Responses were normalized to OW stimulation.

The effects of systematically varying the radial location and separation between VP bipolar electrodes on spatial tuning curves were examined using five electrode positions distributed across the radial dimension of the cochlea (Figure 9). In these experiments, one contact was placed either on the habenula (H) or at a position on the OSL between the habenula and the proximal modiolus (locations labeled H - 0 in Fig. 9). The other contact was placed remotely.

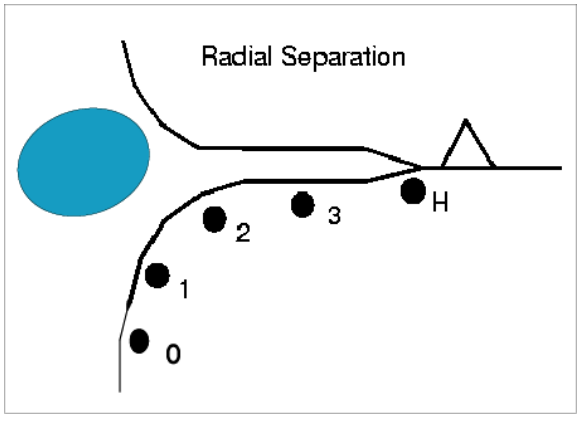

Figure 9. Diagram of five radial electrode placements used with VP radial electrodes to test the effects of different radial electrode placements in the basal cochlea on threshold and spatial spread of evoked activity in the ICC.

The spread of excitation evoked by activation using these varying electrode separations were examined in several animals. Examples of the STIs and STCs evoked by activation of one electrode pair at four radial separations are illustrated in Figure 10. The STIs (upper and middle rows) illustrate the spread of excitation evoked at two stimulus intensities (+4 and +8 dB re threshold) by electrodes at separations 1H, 2H, 3H and 1,2 (Fig. 10). These combinations were chosen to represent the responses evoked by both the closest (H,1 and 1,2) and most widely separated (H,3) electrode pairs at a broad range of stimulus intensities -- most physiological and psychophysical responses to electrical stimuli saturate with a dynamic range of 12 dB (Snyder et al., 1991; McKay et al., 1994; Shannon, 1983). At these stimulus intensities, the responses consist of a single burst of spikes restricted to the three or four recording sites located most deeply in the IC, i.e., the sites with the highest BFs and receiving input from the most basal cochlear locations. The STCs in Figure 10 (Bottom row) summarize the spread of activation for these electrode separations for 20 stimulus intensities. In each case, the spread of activation is restricted to the highest frequency sites even at the highest stimulus levels. These STCs are typical of those evoked using visually placed radial electrode pairs. The spread of excitation evoked by these electrical pulses is equal to or less than that observed with acoustic stimulation. They may be compared to those evoked by a 22 kHz acoustic stimulus (see Figure 6). The position of radial electrodes and the magnitude of their separation appear to have little effect on the spread of activation across the IC (compare the STC for 1,H with that for 3,H), although it has some effect on the absolute threshold of the responses. More widely separated electrode pairs tend to have lower thresholds. Thus, radial electrode separation and radial placement relative to the excitable neural elements has little effect on the spread of excitation along the cochlear spiral.

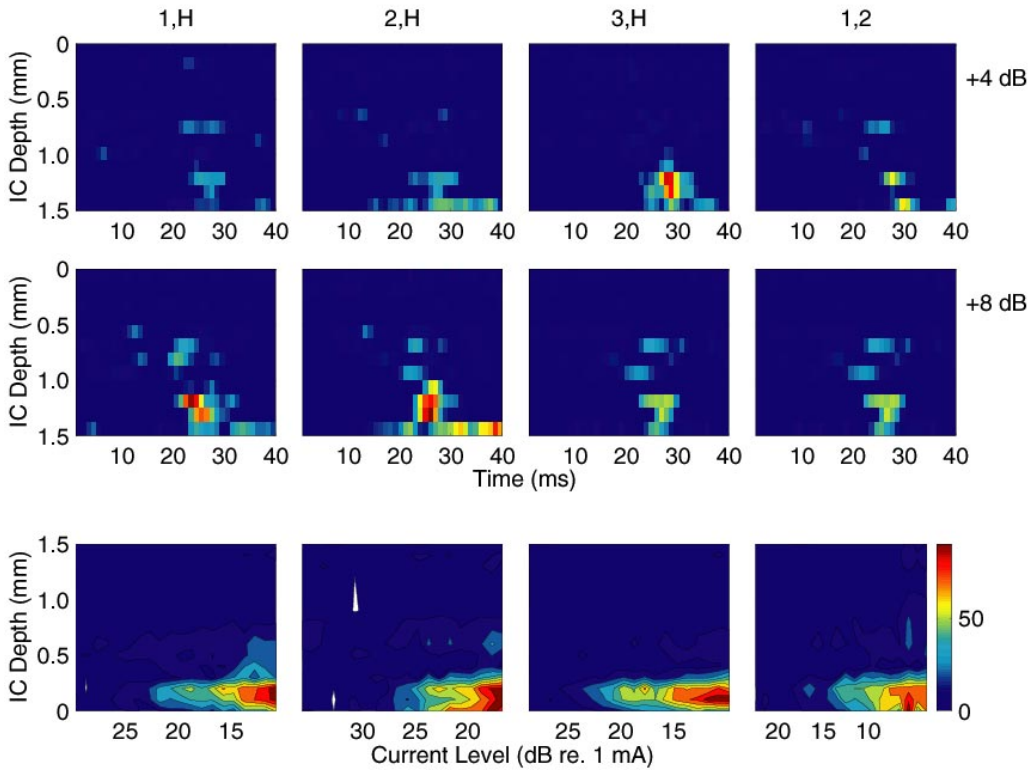

Figure 10: Upper Two Rows: Images of responses obtained in response to pulses at current levels 4 and 8 dB above the threshold for each radial bipolar VP electrode position. In the 3 cases shown in the left 3 columns, one of the electrodes was positioned over the habenula perforata (H) and the other electrode was positioned at sites 1, 2, or 3 (see Fig. 9). In the case shown in the right column, the electrodes were positioned at sites 1 and 2, on either side of the spiral ganglion. **Lower Row:** Spatial tuning curves with iso-rate contours for each electrode position.

Spatial tuning curves illustrating tonotopic shifts of STCs: In contrast to radial placement of electrode pairs, the longitudinal placement of electrodes has a strong effect on the BL and location of maximum activation in STIs and STCs. Figure 11 illustrates visually placed electrodes placed at three locations within the cochlea. Figure 11a shows an STC evoked by activation of a electrode pair placed on the OSL in the second cochlear turn. As expected, the lowest threshold evoked activity occurs at the most superficial (lowest frequency) recording sites (sites 0-7). The BL and region of maximum activation occurs at site 4. When the stimulating electrodes are placed on the apical basal turn, the evoked activity pattern shifted to deeper (higher frequency) IC locations at recording sites centered on site 10. Finally, when these stimulating electrodes were shifted to an even more basal cochlear location within the basal turn, the evoked activity pattern shifted to even deeper IC locations with the BL and region of maximum activation centered at site 14.

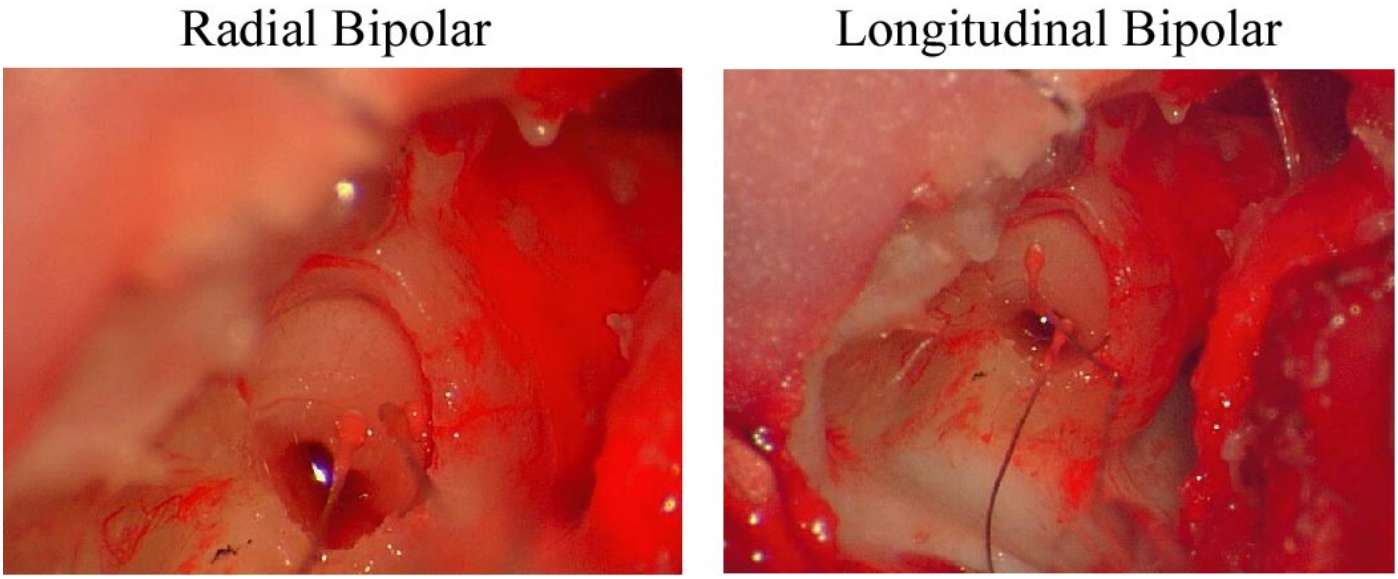

Figure 11: Photographs of visually placed (VP) electrodes in the basal turn of a guinea pig. The photo on the left shows a radially placed VP electrode pair. The photo on the right shows a longitudinally placed VP electrode pair.

In contrast to the small effects on activation spread produced by radial electrode separation and placement, the electrode orientation (radial vs. longitudinal) of bipolar electrodes had a strong influence on activation spread. Figure 11 illustrates the difference between two electrode placements tested. Figure 11A illustrate a radially oriented electrode pair at the basal end of the basal (1st) cochlear turn. The second image(Fig. 11B) illustrates a longitudinal electrode pair in the same cochlea. One electrode of this pair is located at the same cochlear location as that in Figure 11A. The other electrode has been moved basally to the middle of the hook region. The effects on the spread of excitation of these two orientations can be seen in Figure 12, which shows the STIs (left) and STCs (right) evoked by these two placements. Evoked activity produced by electrodes in the radial orientation is restricted to probe site #13, whereas stimulation at the same level in the longitudinal orientation produces activation that is distributed across six sites (#s10 – 16). The STCs evoked by these configurations demonstrate that this difference in activation spread is apparent at all stimulus levels. Stimulation in the radial orientation

produces relatively narrow contours with the region of maximum activation centered on site #13 with only moderate spread to deeper and more superficial locations (corresponding to regions with higher and lower BFs). This restricted activation persists even at stimulus levels 15 dB above threshold. This suggests that the pulses from radially oriented electrode continue to activate the same restricted regions of the auditory nerves array across a wide range of intensities. In contrast, stimulation in the longitudinal orientation produces broad activation contours that spread form site# 13 to site# 10. In addition, the region of maximum excitation, which is centered on the tonotopically appropriate sites (11 & 12) at low stimulus levels, shifts at high stimulus levels to tonotopically inappropriate superficial sites (#s 2 & 4). These results are consistent with the suggestion that longitudinally oriented electrodes promote the invasion of current into the modiolus and the activation of fibers of passage innervating apical cochlear locations.

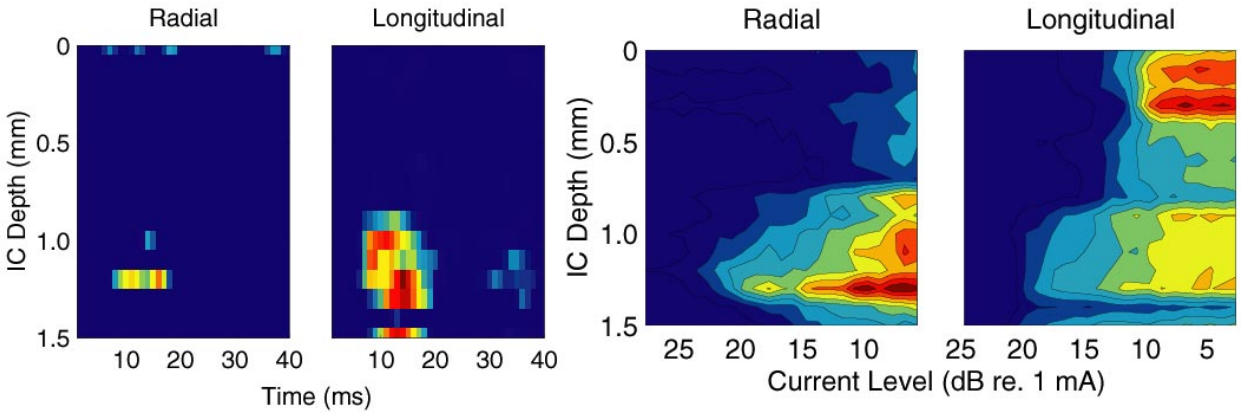

Figure 12. ICC images (left panel) at 2 dB and spatial tuning curves with iso-rate contours (right panel) of activity evoked by radially placed (see Fig. 11A) and longitudinally placed (see Fig 11B) VP electrodes.

A second parameter, which dramatically affects the spatial distribution of activation across the ICC when stimulation is applied using VP electrodes, is stimulation mode (i.e., monopolar vs. bipolar stimulation). Figure 13 illustrates three STCs evoked by stimulation with a radially oriented bipolar electrode pair and those evoked by stimulation of each electrode activated as a monopole (i.e., activated using a remote extracochlear electrode as a return electrode). Stimulation with the radially oriented bipolar electrodes produces restricted activation at all stimulus levels. At near threshold levels the activation is centered on site# 13 and remains centered on this site at higher stimulus levels, although it spreads gradually to adjacent sites at higher stimulus levels and the region of maximum activity shifts slightly to deeper locations. In contrast, monopolar stimulation, using either electrode of the radial pair, produces broad, idiosyncratic patterns of activation. Although the thresholds are much lower and the BL of each pattern is approximately the same as that seen following bipolar stimulation, the activation contours are virtually horizontal stripes stretching across all the sites along the electrode.

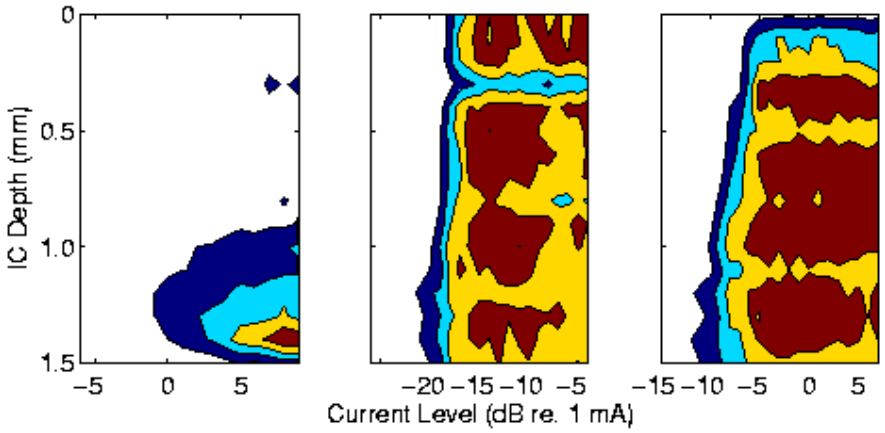

Figure 13. Spatial tuning curves evoked by pulses delivered to the basal turn of guinea pig GP200015. Left panel, bipolar radial VP electrodes. Middle panel, monopolar stimulation with pulses delivered via the modiolar electrode of VP pair on the left. Right panel, oval window vs. habenular electrode of radial pair.

Nucleus Banded Electrodes: In addition to stimulation with visually placed electrodes, we examined the effects of stimulation with models of currently available commercial implants. The first of these that we examined was a modified (shortened) Nucleus (Cochlear Corporation) banded electrode. Figure 14A shows a close-up photograph of the intracochlear end of this electrode. It consists of 6 platinum bands with connecting wires embedded in a silicon elastomer carrier. Figure 14B shows this electrode after it has been inserted in to a guinea pig cochlea through a cochleostomy in the lateral wall of the basal turn.

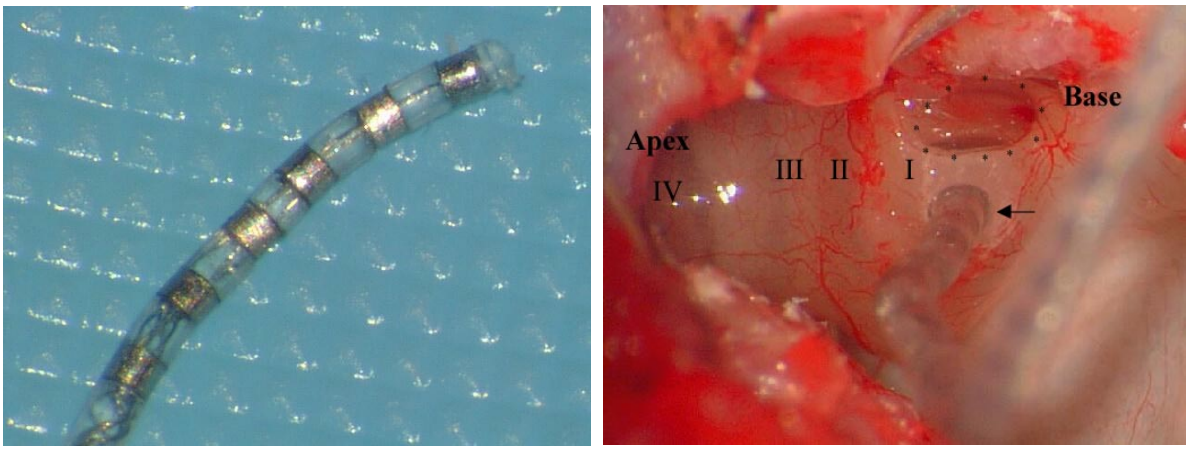

Figure 14. Photographs of a Nucleus banded implant modified for insertion into the guinea pig cochlea. A. The terminal end of the implant showing the six bands. B. The electrode inserted through a cochleostomy (arrow) in the lateral wall of the guinea pig cochlea. All six bands of the implant have been inserted into the cochlea. The lateral wall of the bulla has been removed so that the lateral wall of the cochlea can be seen. The edge of the round window is indicated by the asterisks. The four turns of the guinea pig cochlea are indicated by the roman numerals (I-IV). The base of the cochlea is to the right and the apex is to the left.

Figure 15 illustrates representative examples of STCs evoked by activation of this electrode in three modes: monopolar, i.e., activation of each band with a remote extracochlear electrode acting as the return (upper row), bipolar, i.e., bands activated in pairs (middle row) and tripolar, i.e., activation of a center band with both adjacent bands acting as the return (lower row).

Monopolar activation of any of the bands produced broad, idiosyncratic activation of the ICC. The iso-rate contours are virtually horizontal bands that stretch the entire length of the recording probe. Although these is a tendency for BL and the centroid of excitation to shift ventrally as the more basally located bands are activated (compare MP6, the most apical band, with MP1, the most basal band), monopolar stimulation appears to produce very poor excitation selectivity.

The bipolar configuration (center row) produces activation that is highly variable in threshold and selectivity. This variability can be directly related to the intracochlear location of the bands. Bipolar activation of apically located band pairs (BP5, i.e., activation of bands 5&6) produced low threshold excitation with highly restricted excitation patterns, whereas activation of basally located pairs (BP1, i.e., activation of bands 1&2) produced excitation only at high thresholds and selectivity that is very broad. This difference in threshold and activation selectivity is assumed to be due to the difference in the cross-sectional area of the scala tympani at the different intracochlear locations of the bands. The scala tympani is relatively narrow in the 2nd turn and the apical bands (especially 5&6) are forced to lie close to the modiolus and the spiral ganglion, which it contains. At more basal locations, the scala tympani gradually expands so that it is relatively broad in the hook region. At this location, the bands can reside relatively far from the modiolus and its neural elements. This greater distance presumably accounts for the higher thresholds and poorer excitation selectivity produced by activation of these bands.

Tripolar activation of the bands along the Nucleus implant produced excitation at thresholds that were comparable to those seen with bipolar stimulation and higher than those seen with monopolar stimulation. However, the excitation patterns evoked by tripolar stimulation were much more consistent and more consistently restricted than those seen with bipolar or monopolar stimulation. STCs evoked by tripolar stimulation were among the most restricted observed and were comparable to those seen with radial VP electrodes. As with bipolar stimulation, thresholds for tripolar activation at the most apical location were usually lower than those located more basally, but the spread of excitation did not vary systematically with location along the cochlear spiral.

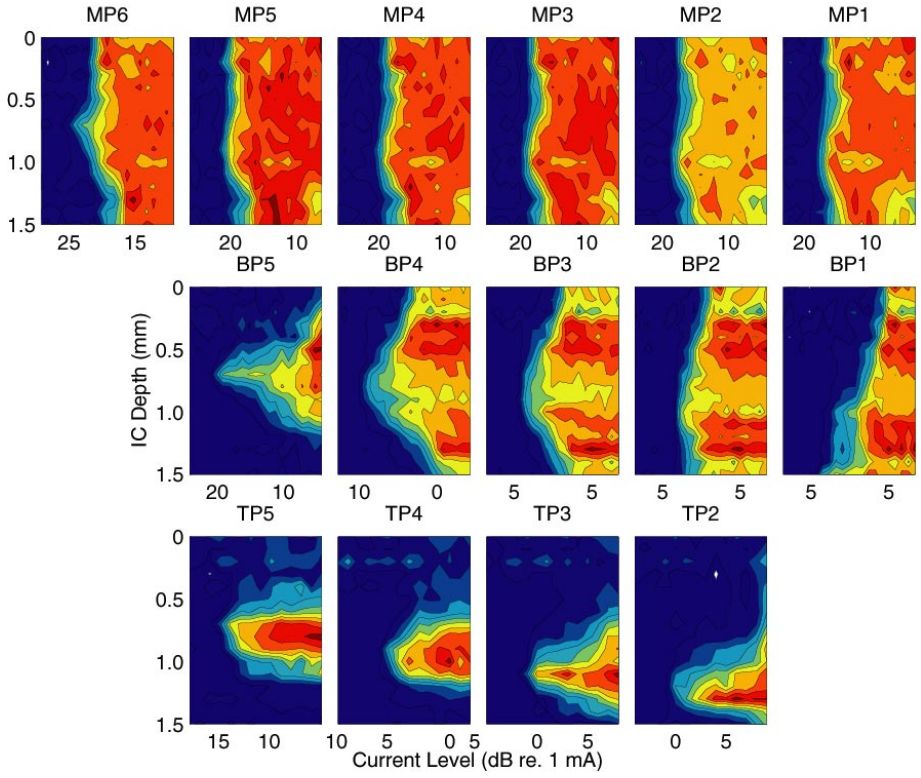

Figure 15. Spatial tuning curves iso-rate contours evoked by activation of a modified Nucleus electrode. Activation of all bands across the entire recording array at current levels 1-2 dB above threshold are illustrated. **Upper Row:** Each band activated and a monopole (MP) electrode. **Middle Row:** Each adjacent pair of electrodes (1,2; 2,3; 3,4 etc.) activated as bipoles (BP). **Bottom Row:** Adjacent triads of electrodes (1,2,3; 2,3,4 etc.) activated as tripoles. Stimuli were biphasic pulses 160 μs/phase. Data are from GP200025.

UCSF Electrodes: In a final set of experiments, we examined the effects of ICES using a UCSF-type cat electrode modified to fit into the guinea pig cochlea. This electrode models many aspects of the Clarion cochlear implant. A drawing of the UCSF electrode is shown in Figure 16A and a photograph of the intracochlear portion of the electrode is shown in Figure 16B. The electrode has four insulated Platinum-Iridium wires, which terminate as ball contacts 250 μm in diameter (labeled 1-4 from apical to basal). All these elements are embedded in a clear silicon elastomer. The 4 contacts are arranged as two off-radial bipolar pairs (1,2 & 3,4). The separation between contacts within these pairs is approximately 1 mm. The pair consisting of contacts 2 & 3 is arranged such that they constitute a longitudinal pair with a separation between them of approximately 2 mm.

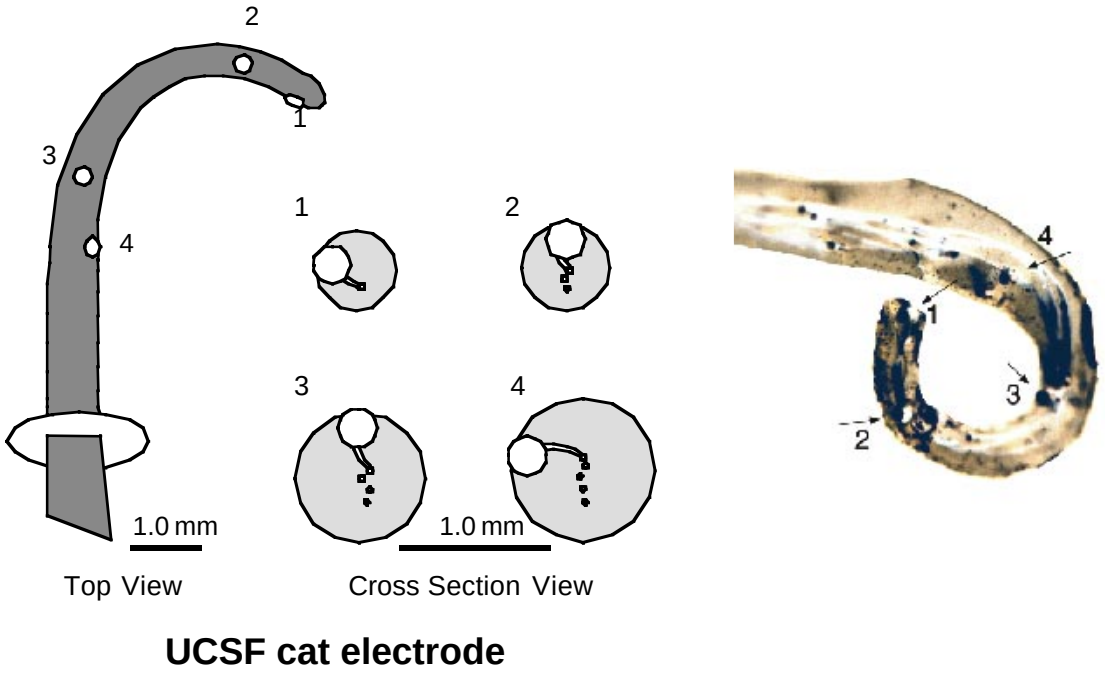

Figure 16. A UCSF cat implant was modified for insertion into the guinea pig cochlear. It has four platinum wires, which end as 200 μm balls embedded in a silastic carrier. Pairs 1-2 and 3-4 each formed off-radial bipolar pairs separated by 1 mm. Pair 2-3 formed a longitudinally bipolar pair separated by 3 mm. The UCSF electrode is similar to the Clarion clinical device.

Figure 17 illustrates representative STCs evoked by activation of the UCSF electrode as monopoles (upper row), as a longitudinal bipolar pair (2,3) and as off-radial bipolar pairs (1,2 & 3,4). Just as with all previous monopolar STCs, monopolar activation of any one of the UCSF contacts (upper row) produces broad excitation across the IC. None of these STCs has a clear BL and the maximum response regions are patchy. The iso-rate contours at low response rates are vertical stripes, which cross all 16 contacts of the recording probe. At higher response rates, the contours break up into idiosyncratic horizontal patches that extend along the domains of individual or multiple recording sites.

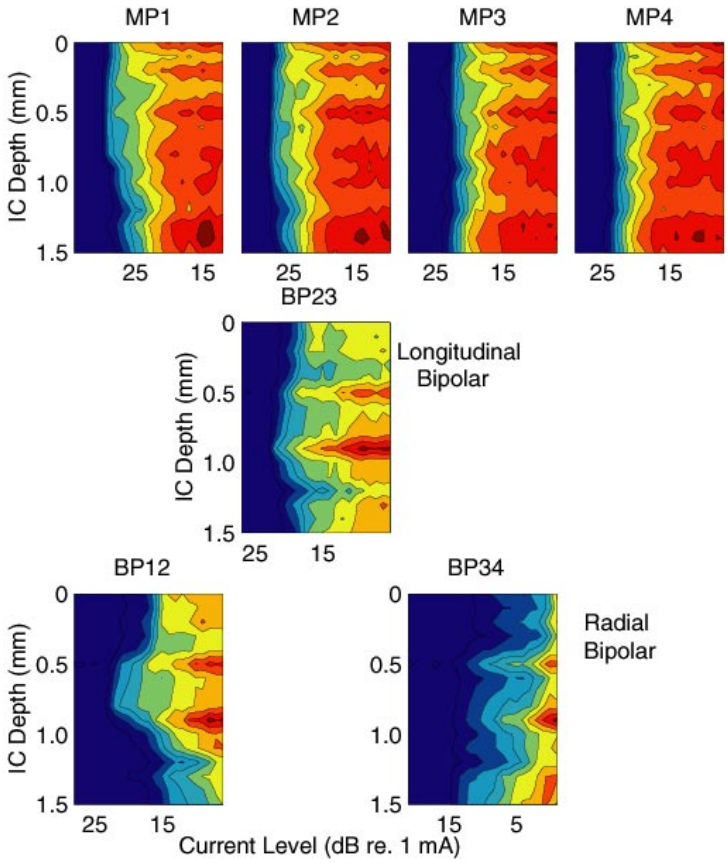

Figure 17. Spatial tuning curves with iso-rate contours evoked by single pulse stimulation of a modified UCSF implant. Activation of all contacts across the entire recording array at current levels 1-2 dB above threshold are illustrated. **Upper Panel**: Each contact was activated as a monopole (MP) electrode. **Middle Panel**: Widely spaced bipolar electrode pair 2,3 activated as a longitudinal bipolar electrode. **Bottom Panel**: Adjacent bipolar electrodes (1,2 and 3,4) activated as off-radial bipolar electrodes. Stimuli were biphasic pulses 160 μs/phase.

Bipolar stimulation of the longitudinal UCSF contacts (pair 2,3) also produces relatively broad activation of the IC. However, in contrast to any of the monopolar STCs, this longitudinal STC shows a clear BL at site#10, 0.9 mm from the proximal end of the probe and two regions of maximum activity, ,ne regionlocated at site#6 or 0.5 mm along the probe, and the other located at site 10. The maximumat 0.5 mm presumably correspond to the region maximally activated by the apical contact and that at 0.9 mm corresponds to the region maximally activated by the basal contact.

Bipolar stimulation of the off-radial contacts (pairs 1,2 and 3,4) of the UCSF electrode produced activation that was somewhat more selective than that produced by activation of the longitudinal contacts (2,3). Their STCs were qualitatively comparable to those produced by bipolar stimulation with the Nucleus bipolar bands. Typically, the STCs evoked by stimulation of pair 1,2, which is located in the more apical scala tympani, have BLs located superficially, usually between 0.5 and 1.0 mm along the probe, which is consistent with their apical location. In addition, these apical STCs have lower thresholds and a more restricted activation patterns than those evoked by activation of basal pair (3,4), which is consistent with apical contacts being forced into closer proximity to the modiolus by the smaller cross-sectional area of the apical scala. The STC produced by activation of the basal off-radial pair (3,4) have a BL located at the deepest sites along the probe, which is consistent with their basal

location, and they have higher thresholds and broader activity patterns, which is consistent with the wider scala tympani at their location. No tripolar stimulation was completed with the UCSF type electrode.

DISCUSSION:

This study examined the effects of electrode placement, orientation and separation as well as stimulation mode (monopolar, bipolar or tripolar) on the spatial distribution of neural activity evoked across the tonotopic organization of the IC in the anesthetized guinea pig. In this study, we have compared the spatial selectivity of evoked activity produced by stimulation of three different types of intracochlear electrodes: visually placed balls, a modified Nucleus 22 implant and a modified UCSF implant. The results of these preliminary experiments lead to the conclusions that: 1) intra-cochlear electrical stimuli, which activate restricted auditory nerve sectors, produce activation of restricted sectors of the cochleotopic representation in the inferior colliculus. 2) Radial bipolar electrode configurations produce more restricted activation patterns than do longitudinal- bipolar or monopolar configurations. 3) The extent of ICC activation is relatively insensitive to the radial separation of radial bipolar pairs. 4) Electrode contacts in the tripolar orientation produced activation patterns that were nearly as restricted as patterns activated by radial bipolar electrodes placed visually, which in turn were nearly as restricted as patterns elicited by tones in normal-hearing animals.

In this Discussion, we will emphasize comparisons of these results with the findings of others using different experimental techniques. In psychophysical studies of human subjects pitch ranking and/or pitch scaling, loudness summation, electrode discrimination, forward masking and gap detection, has been used to estimate channel selectivity in CI users. Most of these behavioral studies have inferred good selectivity in most users. Even the earliest psychophysical studies reported orderly shifts in pitch percepts with electrode activation at successive cochlear locations (Eddington et al, ’78, Tong et al, ’82; Shannon, ’83, Tong and Clark, ’85, Townshend et al, ’87; Nelson et al, ’95; Busby et al, ‘94). *Some* CI users are reported to be able to distinguish between many or all adjacent electrode pairs throughout the length of their electrode (Towshend et al, ‘87; McDermott and McKay, ’94; McKay et al 2000; Pfingst et al, 2000) and *some* report an orderly progression of pitch percepts when successive electrode contacts were activated.

However, most of these studies also reported wide variation amongCI users in their ability to assign specific pitch percepts to activation of different electrode contacts. They also report wide variability in the user’s ability to discriminate between contacts. Some users cannot discriminate between even widely separated contacts (Townshend, ’87; McDermott and McKay, ’94), and others reported no change in pitch (or even pitch reversals) with activation at several successive electrode locations (Shannon, ’83, Townshend, ’87; McDermott and McKay, ’94).

These inter-subject differences have led some investigators to emphasize that the pitch percepts evoked by even carefully loudness-balanced electrical stimuli are weak, complex and multidimensional (Shannon, ’83; Collins et al ‘97). They conclude that this complexity may be derived from several sources including electrode placement anomalies (see Ketten et al, ’98; Wardrop et al, 2001); irregular patterns of current spread, and irregularities in spiral ganglion cell survival and threshold. All of these factors could lead to broad and/or irregular patterns of activation within the auditory nerve.

Variability in evoked pitch percepts and difficulties in the interpretation of electrode discrimination studies have led to the use of other psychophysical procedures to estimate channel selectivity and channel interaction. These additional procedures have included forward masking (Lim et

al, ’89; Chatterjee and Shannon, ’98; Tong and Clark, ’86), gap detection (Chatterjee et al 1998, Hanekom and Shannon, 1998) and loudness summation (Tong and Clark, ’86). Although none of these methods has provided an unequivocal measure of the intracochlear spread of excitation (Hanekom and Shannon, ’98; Chatterjee and Shannnon, ’98), some have emphasized that the inferred activation patterns could be highly selective, as selective as those evoked acoustically (see Fig. 12, Chatterjee and Shannon, 1998). However, even these results must be interpreted with caution, since the acoustic activation (i.e., 1 kHz tones at 70 dB SPL), which was used as the acoustic comparison, actually produces very broad activation of the auditory nerve array (Kim and Molnar, 1974).

In addition to psychophysical studies of activation selectivity, several modeling studies have attempted to define the intracochlear spread of current in cochlear implants. The approaches used in these studies range from saline tank/ resistive network models of voltage distributions within the cochlea (Strelioff , 1973; Black and Clark, 1980; Black et al, 1981; O’Leary et al, 1985; Girizon, 1987; Ifukbe and White, 1987; Kasper et al., 1991; Suesserman and Spelman, 1993; Jolly et al, 1996; Kral et al, 1998) to 2-D and 3-D computer simulations of intracochlear stimulation. These computer simulations attempt to model *in vivo* spatial excitation patterns produced by single electrodes in the spiral of the auditory nerve array (Finley et al, 1987; 1990; Frijn et al, 1995, 1996; Rattay et al., 2001a,b). Some of these models predict highly restricted distributions of intracochlear current and subsequent patterns of auditory nerve activation (e.g., Frijn et al, 1995, 1996, Finley et al, 1990; Rattay et al., 2001b), especially when the electrodes are activated as intracochlear bipolar (or tripolar) pairs. However, other models predict broad complicated patterns of current spread in many activation modes including bipolar stimulation (Jolly et al., 1996; Ifukube and White, 1987; Black et al, 1981).

Physiological estimates of current spread and activation selectivity have been conducted *in vivo* in two types of experiments: direct observations of selectivity in the auditory nerve and indirect observations based of spread of activation across tonotopic organization of central auditory nuclei. Direct physiological observations on activation selectivity were made *in hearing cats* (van den Honert and Stypulkowski, 1987; Kral et al. 1998). These studies reported a broad range of selectivity depending upon the intracochlear electrode orientation(monopolar, bipolar, or tripolar; radial or longitudinal) and stimulus polarity (cathodal or anodal first). They reported highly selective activation using radially oriented, bipolar (and tripolar) electrodes and poor selectivity using monopolar stimulation (activation of a single electrode relative to an extracochlear return electrode).

Indirect estimates of intracochlear current spread and patterns of intracochlear activation have been reported in numerous studies using evoked activity across central auditory nuclei to infer intracochlear activation. These studies measuredthe distribution of electrically evoked activity across central auditory areas and compared those distributions, either explicitly or implicitly, with tone-evoked activity distributions, which were usually recorded in other animals. Several of these studies have examined the distribution of electrically evoked activity across the tonotopically organized central nucleus of the inferior colliculus, ICC (Merzenich et al., 1974,1979; Snyder et al., 1990,1991; Ryan et al., 1990; Brown et al., 1992; Sheperd et al., 1999; Leake et al., 2000; Moore et al. 2001; Rescher et al., 2001). Others have made similar measurements across primary auditory cortex (Klinke et al., 1999; Raggio and Schreiner, 1999; Arenberg and Middlebrooks, 2000, 2001).

Comparisons of results across these physiological studies to determine the factors governing stimulus selectivity are difficult. Each study often uses a single, and unique stimulation paradigm. They use different intracochlear electrode types. These electrodes include modified Nucleus™ electrodes (a series of longitudinally arrayed bands on a cylindrical silicone carrier), modified UCSF or Clarion™ electrodes (a series of ball electrodes on a tapered silicone carrier), or simple wire-and-ball electrodes (independently placed balls with no silicone carrier). They use different electrode orientations

(longitudinal, radial or off-radial), and they use different stimulation configurations (monopolar, bipolar or tripolar). In addition, these studies use animals in which the mode and durations of deafness is highly variable. This in turn leads to variability in percentage survival of auditory nerve fibers. Thus, the reported results are highly variable both within and between studies. Some studies report highly restricted evoked-activity patterns, which reflect the topographic organization of the cochlea and its central connections and which are comparable to patterns evoked by acoustic stimuli (Snyder et al., 1990; Ryan et al., 1990; Brown et al., 1992). Others report broad and/or idiosyncratic activation patterns (Rebscher et al., 2001; Kral et al., 1998; Shepherd et al., 1999; Raggio and Schreiner, 1999).

ACKNOWLEDGMENTS

This work was supported NIH grants RO1 DC04312 (JCM), RO1 DC03549 (RLS), NCRR grant P41-RR09754 and contract N01-DC-7-2107 (RLS). We thank Chris Ellinger, Shigeto Furukawa and Zekiye Onsan for their technical support and Steve Rebscher for making the UCSF electrode. Multi-channel recording probes were generously provided by the University of Michigan Center for Neural Communication Technology, University of Michigan (www.engin.umich.edu/facility/cnct, which is supported by NIH/NCRR grant P41-RR09754.

REFERENCES

Arenberg JG, Middlebrooks JC (2000) Cortical responses to multi-channel auditory prosthesis stimulation. 23rdMidwinter Meeting of the Association of Research in Otolaryngology, St. Petersburg Beach, FL, February 2000.

Arenberg JG, Furukawa, S, Middlebrooks JC (2000) Auditory cortical images of tones and noise bands. J. Assoc. Res. Oto. 1:183-194.C

Aitkin, L. (1986) The Auditory Midbrain: Structure and Function in the Central Auditory Pathway. Humana Press, New Jersey.

Batra, R., Kuwada, K., Stanford, TR. (1989) Temporal coding of envelopes and their interaural delays in inferior colliculus of the unanesthetized rabbit. J. Neurophysiol., 61:257-268.

Bierer, JA, Snyder, RL, Middlebrooks, JC. (2001) Patterns of inferior colliculus activity in response to intracochlear electrical stimulation. 24th Midwinter Meeting of the Association of Research in Otolaryngology, St. Petersburg Beach, FL,

Bierer, JA, Middlebrooks, JC (2001) Auditory cortical images of cochlear- implant stimuli: Dependence on electrode configuration. J Neurophysiol.(in press)

Bierer, JA, Snyder, RL, Middlebrooks, JC. (2002) Patterns of inferior colliculus activity in response to intracochlear electrical stimulation. 24th Midwinter Meeting of the Association of Research in Otolaryngology, St. Petersburg Beach, FL,

Black, RC, Clark, GM. (1980) Differential electrical excitation of the auditory nerve. J Acoust. Soc. Am. 67:868-874.

Black, RC, Clark, GM, Patrick, JF. (1981) Current distribution measurements with the human cochlea. IEEE Trans. Biomed. Eng. BME-28: 721-725.

Black, RC, Clark, GM., Tong, YC, Patrick, JF. (1983) Current distribution in cochlear stimulation. Ann. N.Y. Acad. Sci. 405:137-145.

Brown, CJ, Shepherd, RK, Webster, WR, Martin, RL, Clark, GM. (1992) Cochleotopic selectivity of a multichannel scala tympani electrode array using the 2-deoxyglucose technique. Hear. Res. 59:224-240.

Brown, CJ, Abbas, PJ, Borland, J, Bertschy, MR. (1996) Electrically evoked whole nerve action potentials in Ineraid Auditory prosthesis users: responses to different stimulation electrode configurations and comparisons to psychophysical responses. J. Speech Hear. Res. 39:453-467.

Burns, EM, Viemeister, NF. (1976) Nonspectral pitch. J. Acoust. Soc. Am. 60:863-869.

Busby, PA, Whitford, LA, Blamey, PJ, Richardson, LM, Clark, GM (1994) Pitch perception for different modes of stimulation using the cochlear multiple-electrode prosthesis. J. Acoust. Soc. Am. 95:2658-2669.

Chatterjee, M, Shannon, RV (1998) Forward masked excitation patterns in multielectrode electrical stimulation. J. Acoust. Soc. Am. 103:2565-72.

Chatterjee, M, Fu, QJ, Shannon, RV (1998) Within-channel gap detection using dissimilar markers in auditory prosthesis listeners. J. Acoust. Soc. Am. 103:2515-9.

Chatterjee, M. (1999) Temporal mechanisms underlying recovery from forward masking in multielectrode-implant listeners. J. Acoust.Soc. Am. 105:1853-1863.

Chen, GD, Sinex, DG**. (**1999) Effects of interaural time differences on the responses of chinchilla inferior colliculus neurons to consonant-vowel syllables. Hear. Res. 138(1-2): 29-44.

Chen, GD, Nuding, SC, Narylyan, SS, Sinex, DG (1996) Responses of ingle neurons in the chinchillar inferior colliculus to sonsonant-vowel syllables differing in voice onset time. Audit. Neurosci. 3: 179-198.

Collins, LM, Zwolen, TA, Wakefield, GH (1997) Comparison of electrode discrimination, pitch ranking, and pitch scaling data in postlingually deaf aduslt auditory prosthesis subjects. J. Acoust. Soc. 101:440-455.

Davis, H., Silverman, SR. (1978) Hearing and Deafness (Holt, Rinehart and Winston, New York).

Delgutte, B, Hammond, DM, Cariani, PA. (1998) Neural coding of the temporal envelope of speech: Relation to modulation transfer functions. In: Psychophysical and Physiological Advances in Hear.. Palmer, AR, Rees, A, Summerfield, Q, and Meddis, R, eds. Whurr, London. pp 595-603.

Delgutte, B, Kiang, NYS. (1984) Speech coding in the auditory nerve: I. Vowel-like sounds. J. Acoust. Soc. Am. 75:866-878.

Drake KL, Wise KD, Farraye J, Anderson DJ, BeMent SL (1988) Performance of planar multisite microprobes inrecording extracellular single-unit intracortical activity. IEEE Trans. Biomed. Eng. BME-35:719-732

Dynes, SBC. (1996) Discharge characteristics of auditory nerve fibers for pulsatile electrical stimuli. MIT Doctoral Dissertation.

Dynes, SBC, Delgutte, B. (1992) Phase-locking of auditory-nerve discharges to sinusoidal electrical stimulation of the cochlea. Hear. Res. 58:79-90.

Efron, B, Tibshirani, R (1991) Statistical data analysis in the computer age. Science 253:390-395

Eddington, DK, Dobelle, WH, Brackman, DE, Mladejovsky, MG, Parkin, JL (1978) Auditory prosthesis research with multiple channel intracochlear stimulation in Man. Ann. Otol. Rhinol. Laryngol. 87(Suppl 53):1-39.

Finley, CC. (1989). "A Finite-Element Model of Radial Bipolar Field Patterns in the Electrically Stimulated Cochlea - Two and Three Dimensional Approximations and Tissue Sensitivities." IEEE -11th Ann. Int. Conf. Eng. Med. Biol. Soc.1059-1060.

Finley, CC, Wilson, BS, White, MW. (1987). A Finite-Element Model of Bipolar Field Patterns in the Electrically Stimulated Cochlea - a Two Dimensional Approximation. IEEE - Ninth Ann. Conf. Eng. Med. Biol. Soc.1901-1903.

Finley, CC, Wilson, BS, White, MW. (1990) Models of neural responsiveness to electrical stimulation. In: Miller, J.M., Spelman, F.A., eds. Auditory prostheses: Models of the Electrically Stimulated Ear. Springer, N.Y. pp 55-96.

Friesen, LM, Shannon, RV, Baskent, D, Wang, X. (2001) Speech recognition in noise as a function of the number of spectral channels: Comparison of acoustic hearing and cochlear implants. J. Acoust. Soc. Am. 110:1150-1163.

Frijns, JHM, Kate, JHT. (1994) A Model of Mylinated Nerve Fibers for Electrical Prosthesis Design. Med.Biol.Eng.Comput. 32**:**391-398.

Frijns, JHM, Mooij, J, Kate, JHT. (1994). A Quantitative Approach to Modeling Mammalian Myelinated Nerve Fibers for Electrical Prosthesis Design. IEEE Trans.Biomed.Eng. 41**:**556-566.

Frijns, JHM, Snoo, SL d, Kate, JHT. (1996). Spatial Selectivity in a Rotationally Symmetric Model of the Electrically Stimulated Cochlea. Hear Res 95**:**33-48.

Frijns, JHM., Snoo, SL d, Schoonhoven, R. (1995). Potential Distributions and Neural Excitation Patterns in a Rotationally Symmetric Model of the Electrically Stimulated Cochlea. Hear Res 87**:**170-186.

Furukawa S; Xu L; Middlebrooks JC. (2000) Coding of sound-source location by ensembles of cortical neurons. J. Neuroscience. 20:1216-1228.

Gaese, BH. Ostwald J (2001) Anesthesia Changes Frequency Tuning of Neurons in the Rat Primary Auditory Cortex. J. Neurophysiol. 86: 1062-1066.

Girzon, G. (1984) Investigation of current flow in the inner ear during electrical stimulation of intracochlear electrodes. M.S.E.E. thesis, Massachusetts Institute of Technology. Cambridge, MA.

Glass, I. (1983) Tuning characteristics of cochlear nucleus units in response to electrical stimulation of the cochlea. Hear. Res. 12:223-237.

Greenwood, D.D. (1974) Critical bandwidth in man and some other species in relation to the traveling wave envelope. In: H.R. Moskowitz and J.C. Stevens (eds): Sensation and Measurement. Boston: Reidel, pp. 231-239.

Hanekom JJ, Shannon RV. (1998) Gap detection as a measure of electrode interaction in auditory prostheses. J. Acoust. Soc. Am. 104:2372-84.

Hartmann, R. and Klinke, R. (1989) Response characteristics of nerve fibers to patterned electrical stimulation. In: Auditory prostheses: Models of the Electrically Stimulated Ear. eds. J.M.Miller and F.A.Spelman, pp. 135-160, New York, Springer-Verlag.

Ifukube, T, White, RL. (1987) Current distributions produced inside and outside the cochlea from a scala tympani electrode array. IEEE Trans. Biomed. Eng. 34:883-890.

Javel, E (1989) Acoustic and electrical encoding of temporal information. In: Auditory prostheses: Models of the Electrically Stimulated Ear. Miller, JM, Spelman, FA, eds. Springer-Verlag, New York.

Johnson, DH. (1980) The relationship between spike rate and synchrony in responses of auditory-nerve fibers to single tones. J. Acoust. Soc. Am. 88:1115-1122.

Jolly, CN, Spelman, FA, Clopman, BM. (1996) Quadrapolar stimulation of cochlear prostheses: modeling and experimental data. IEEE Trans. Biomed. Eng. BME-43, 857-865.

Joris, PX, Yin, TCT. (1992) Responses to amplitude-modulated tones in the auditory nerve of cats. J. Acoust. Soc. Am. 91:215-232.

Kasper, A., Pelizzoni, M., Montandon, P. (1991) Intracochlear potential distribution with intracochlear and extracochlear electrical stimulation in humans. Ann. Otol. Rhinol. Laryngol. 100: 812-816.

Ketten, DR, Skinner, MW, Wang, G, Vannier, MW, Gates, GA, Neely, JG (1998) In vivo measures of cochlear length and insertion depth of nucleus auditory prosthesis electrode arrays. Ann Otol Rhinol Laryngol 107:1-16.

Killian, MJP, Klis, SFL, Smoorenburg, GF. (1994) Adaptation in the compound action potential response of the guinea pig VIIIth nerve to electrical stimulation. Hear. Res. 81:66-82.

Kim, DO, Molnar, CE. (1979) A population study of cochlear nerve fibers: Comparison of spatial distributions of average-rate and phase-locking measures of responses of single tones. J. Neurophysiol. 42:16-30.

Klinke, R, Kral, A, Heid, S, Tillein, J, Hartmann, R. (1999) Recruitment of the auditory cortex in congenitally deaf cats by long-term cochlear electrostimulation. Science 285: 1729-1733.

Kohonen, T. *Self-Organization and Associative Memory*. Berlin, Springer-Verlag, 1987.

Kral, A., Hartmann, R., Mortazavi, D., Klinke, R. (1998) Spatial resolution of auditory prostheses: The electrical field and excitation of auditory afferents. Hear. Res. 121: 11-28

Kuwada S, Batra R, and Stanford TR. (1989) Monaural and binaural response properties of neurons in the inferior colliculus of the rabbit: effects of sodium pentobarbital *J Neurophysiol* 61: 269-282.

Langner, G. and Schreiner, CE. (1988) Periodicity coding in the inferior colliculus of the cat. I. Neuronal mechanisms. J. Neurophysiol., 60:1799-1822.

Leake PA, Snyder RL, Hradek, GT, Rebscher SJ. (1995) Consequences of chronic extracochlear electrical stimulation in neonatally deafened cats. Hear. Res. 82:65-80.

Leake, PA, Hradek, GT, Snyder, RL.. (1999) Chronic electrical stimulation with a auditory prosthesis prevents degeneration of spiral ganglion neurons in neonatally deafened cats. J. Comp. Neurol. 412:543-562

Leake PA, Snyder RL, Rebscher, SJ, Moore, CM, Vollmer, M. (2000) Plasticity in central representations in the inferior colliculus induced by chronic single- vs. two-channel electrical stimulation by a auditory prosthesis after neonatal deafness. Hear. Res. 147:221-41.

Liberman, MC. (1982) The cochlear frequency map for the cat: Labeling auditory-nerve fibers of known characteristic frequency. J. Acoust. Soc. Am. 72:1441-1449.

Lim, HH, Tong, YC, Clark, GM (1989) Forward masking patterns produced by intracochlear electrical stimulation of one and two electrode pairs in the human cochlea. J. Acoust. Soc. Am. 86:971-980.

Matsuoka, AJ, Abbas, PJ, Rubinstein, JT, Miller, CA. (2000) The neural response to electrical constant-amplitude pulse train stimulation: evoked compound action potential recordings. Hear. Res. 149:115-128.

Mawman, DJ, Giles, EC, Woolford, TJ, O'Driscoll, M, Hamrouge, S, Ramsden, RT (2000) Telephone use by auditory prosthesis users in Manchester. In: Auditory prostheses, S.B. Waltzman and N.L. Cohen, eds., Thieme, New York pp. 341-342.

May BJ, and Sachs MB. (1992) Dynamic range of neural rate responses in the ventral cochlear nucleus of awake cats. J Neurophysiol 68: 1589-1602.

McDermott, H.J., McKay, C.M., Vandali, A.E. A new portable sound for the University of Melbourne/Nucleus Limited multielectrode auditory prosthesis. J. Acoust. Soc. Am. 91: 3367-3372, 1992.

McDermott, HJ, McKay, CM (1994) Pitch ranking with non-simultaneous dual-electrode electrical stimulation of the cochlea. J. Acous Soc. Am. 96:155-162.

McKay, C.M., O'Brien, A., James, C.J. (1999) Effects of current level on electrode discrimination in electrical stimulation. Hear. Res. 136:159-164.

Merzenich, MM., Schindler, DN, White, MW. (1974) "Auditory prosthesis. The Interface Problem." Biomed. Eng. Instrum. Fund. Electr.Stimul. **3:**321-340.

Merzenich, M.M, White, MW. (1977) Symposium on auditory prostheses: II. The interface problem." Biomed. Eng. Instrum. Fund. Electr. Stimul. **3:**321-340.

Middlebrooks JC; Xu L; Eddins AC; Green DM. (1998) Codes for sound-source location in nontonotopic auditory cortex. J. Neurophysiology. 80:863-81.

Middlebrookes, JC, Bierer, JA. (2001) Auditory cortical images of cochlear-implant stimuli: Coding of stimulus channel and current level. J. Neurophysiol. (in press).

Miller, CA, Abbas, PJ, Rubenstein, JT, Robinson, BK. (2001) Response properties of the refractory auditory nerve fiber. Fifth Quarterly progress report. NIH contract N01-DC-9-2107 The Neurophysiology of simulated auditory prosthesis stimulation.

Miller, GA, and Nicely, PE. An analysis of perceptual confusions among some English consonants. J. Acoust. Soc. Am. 27: 338-352, 1955.

Moore, C.M., Vollmer, M., Leake, P. A., Snyder, R.L., Rebscher, S.J. (2001) Alterations in spatial selectivity of the inferior colliculus following chronic intracochlear stimulation with a auditory prosthesis in adult deafened animals. Hear. Res. (in press).

Najafi K, Wise KD, Mochizuki T (1985) A high-yield IC-compatible multi-channel recording array. IEEE Trans. Electron. Dev. 32:1206-1211

Nelson, DA, Van Tasell, DJ, Schroder, AC, Soli, S, Levine, S (1995) Electrode ranking of 'place pitch' and speech recognition in electrical Hear.. J. Acoust. Soc. Am. 98:1987-1999.

Nuding, SC, Chen, GD, Sinex, DG. **(**1999) Monaural response properties of single neurons in the chinchilla inferior colliculus. Hear. Res 131: 89-106.

O'Leary, S.J., Black, R.C., Clark, G.M. (1985) Current distributions in the cat cochlea: A modeling and electrophysiological study. Hear. Res. 18:273-281.

Parkins, CW. (1989) Temporal response patterns of auditory nerve fibers to electrical stimulation in deafened squirrel monkeys. Hear. Res., 41:137-168

Pfingst, BE, Holloway, LQA, Zwolan, TA, Collins, L.M (1999) Effects of stimulus level on electrode-place discrimination in human subjects with auditory prostheses. Hear. Res. 134:105-115.

Phillips DP, Semple MN, Calford MB, Kitzes LM (1994) Level-dependent representation of stimulus frequency in cat primary auditory cortex. Exp. Brain Res. 102:210-226

Pinker, S, Bloom, P. (1990) Natural language and natural selection. Behavioral and Brain Sciences, 13, 707-784.

Raggio, MW, Schreiner CE. (1999) Neuronal responses in cat primary auditory cortex to electrical cochlear stimulation. III. Activation patterns in short- and long-term deafness. J. Neurophysiol. 82:3506-26.

Ramachandran, R, Davis, KA, May, BJ. (1999) Single-unit responses in the inferior colliculus of decerebrate cats. I. Classification based on frequency response maps. J. Neurophysiol. 82: 152–163.

Rattay, R., Richardson, NL., Felix, H. (2001) A model of the electrically excited cochlear neuron. I. Contribution of neural substructures to the generation and propagation of spikes. Hear. Res. 153: 43-63.

Rattay, R., Richardson, NL., Felix, H. (2001) A model of the electrically excited cochlear neuron. II. Influence of the three-dimensional cochlear structure on neural excitability. Hear. Res. 153: 64-79.

Rebscher, SJ, Snyder, RL, Leake, PA (2001) The effect of electrode orientation on threshold and selectivity of responses to intracochlear electrical stimulation. J. Acoust. Soc. Am. 109:2035-2048.

Rebscher, S.J., P.J. Wardrop, P.A. Leake. (2000). Second Generation Auditory prosthesis Electrodes: Relating the Incidence, Location and Severity of Trauma with Mechanical Aspects of Electrode Design. 5th European Symposium on Peadiatric Auditory prosthesisation, Antwerp Belgium.

Rees, A. and Moller, A.R. (1983) Responses of neurons in the inferiorcolliculus of the rat to AM and FM tones. Hear. Res., 27:129-143.

Rees, A., Møller, AR. (1987) Stimulus properties influencing the responses of inferior colliculus neurons to amplitude-modulated sounds. Hear. Res. 27: 129-143.

Relkin, EM, Turner, CW. (1988) A reexamination of forward masking in the auditory nerve. J.Acoust. Soc. Am. 84:584-91.

Rosen, S. (1992) Temporal information in speech: acoustic, auditory and linguistic aspects. Phil. Trans. R. Soc. Lond. B. 336:367-373.

Rubinstein, JT, Miller, CA. (1999) How do auditory prostheses work? Current Opinion in Neurobiol. 9:399-404.

Rubinstein, JT, Wilson, BS, Finley, CC, Abbas, PJ. (1999) Pseudospontaneous activity: stochastic independence of auditory nerve fibers with electrical stimulation, Hear. Res. 127:108-118

Rumelhart DE, Hinton GE, Williams RJ (1986) Learning internal representations by error propagation. In: Parallel Data Processing.. M.I.T. Press, Cambridge, MA, pp 318-362

Ryan, AF, Miller, JM, Wang, Z-X, Wolf, NK. (1990) Spatial distribution of neural activity evoked by electrical stimulation of the cochlea. Hear. Res. 50:57-70.

Schreiner CE, Mendelson JR, Sutter ML (1992) Functional topography of cat primary auditory cortex: representation of tone intensity. Exp. Brain Res. 92:105-122

Schreiner, CE, Raggio, M. (1996) Neural responses in cat primary auditory cortex to electrical cochlear stimulation. II. Repetition rate coding. J. Neurophysiol. 75:1283-1300.

Schreiner, CE, Urbas, JV. ((1986) Representations of amplitude modulation in the auditory cortex of the cat. I. Anterior auditory field. Hear. Res. 21:227-241

Shannon, RV (1983) Multi-channel electrical stimulation of the auditory nerve in man. I. Basic psychophysics. Hear. Res. 11:157-189.

Shannon, RV. (1990) Forward masking in patients with auditory prostheses. J. Acoust. Soc. Am. 88:741-744.

Shannon, RV. (1991) Temporal modulation transfer functions in patients with auditory prostheses, J.Acoust. Soc.Am, 91:1974-1982.

Shannon, RV, Zeng, F-G, Kamath, V,, Wygonski, J., Ekekid, M. (1995) Speech recognition with primarily temporal cues. Science 270:303-304.

Shepherd, RK, Javel,E. (1997) Electrical stimulation of the auditory nerve: I. Correlation of physiological responses with cochlear status. Hear. Res. 108:112-144.

Shepherd, RK, Baxi, JH, Hardie, NA. (1999) Response of inferior colliculus neurons to electrical stimulation of the auditory nerve in neonatally deafened cats. J. Neurophysiol. 82: 1363-1380.

Shower EG, Biddulph R (1931) Differential pitch sensitivity of the ear. J. Acoust. Soc. Am. 3:275-287

Sinex, DG, Chen, GD. (2000) Neural responses to the onset of voicing are unrelated to other measures of temporal resolution. J. Acoust. Soc. Am. 107(1):486-495.

Sinex, DG, Geisler, CD. (1983) Responses of auditory nerve fibers to consonant-vowel syllables. J. Acoust. Soc. Am. 73, 602-615.

Sinex, DG, Geisler, CD. (1984) Comparison of the responses of auditory nerve fibers to consonant-vowel syllables with predictions from linear models. J. Acoust. Soc. Am. 76, 116-121.

Sinex, DG, McDonald, LP. (1988) Average discharge rate representation of voice-onset time in the chinchilla auditory nerve. J. Acoust. Soc. Am. 83, 1817-1827.

Sinex, DG, McDonald, LP. (1989) Synchronized discharge rate representation of voice-onset time in the chinchilla auditory nerve. J. Acoust. Soc. Am. 85, 1995-2004.

Smith, RL (1977) Short term adaptation in single auditory nerve fibers: some post-stimulatory effects. J Neurophysiol. 40:1098-1112.

Smith, RL. (1979) Adaptation, saturation and physiological masking in single auditory-nerve fibers. J. Acoust. Soc. Am. 65, 166–178.

Smith, RL, Brachman, ML. (1982) Adaptation in auditory-nerve fibers: a revised model. Biol. Cybern. 44:207-120.

Snyder, RL, Rebscher , SJ, Cao, K, Leake, PA, Kelly, K. (1990) Chronic intracochlear electrical stimulation in the neonatally deafened cat. I. Expansion of central representation. Hear. Res 50:7-33.

Snyder, RL, Rebscher, SJ, Leake, PA, Kelly K, Cao K (1991) Chronic intracochlear electrical stimulation in the neonatally deafened cat. II: Temporal properties of neurons in the inferior colliculus. Hear. Res. 56**:**246-264.

Snyder, R.L., P.A. Leake, S. J. Rebscher and R. Beitel. (1995) Effects of neonatal deafening and chronic intra-cochlear electrical stimulation on temporal resolution of cat IC neurons. J. Neurophysiol. 73:449-467.

Snyder, R.L., .M. Vollmer, C. Moore, S. Rebscher, P. A. Leake, R. Beitel. (2000) Responses of inferior colliculus neurons to amplitude modulated intracochlear electrical pulses in deaf cats. J. Neurophysiol. 84:166-184.

Snyder,RL, Bierer, JA, Middlebrooks, JC. (2002) Patterns of inferior colliculus activity in response to acoustic and intracochlear electrical stimulation: Activation selectivity. (appendix)

Strelioff, D. (1973) A computer simulation of the generation and distribution of cochlear potentials. J. Acoust. Soc. Am. 54:620-629.

Suesserman, MF, Spelman, FA. (1992) Lumped-Parameter model for in vivo cochlear stimulation. IEEE Trans. Biomed. Eng. 40: 237-245.

Tillman TW and Carhart T (1966) An expanded test for speech discrimination utilizing CNC monosyllabic words: Northwestern University Auditory Test No. 6. Technical Report No. SAM-TR-66-55, USAF School of Aerospace Medicine, Brooks Air Force Base, Texas.

Tong, YC, Clark, GM (1985) Absolute identification of electric pulse rates and electrode postions by auditory prosthesis patients. J. Acoust. Soc. 77:1881-1888.

Tong, YC, Clark, GM, Blamey, PJ, Busby, PA, Dowell, RC (1982) Psychophysical studies for two multi-channel auditory prosthesis patients. J. Acoust. Soc. Am. 71:153-180.

Townshend, B, Cotter, Compernolle, N, White, RL. (1987) Pitch perception by auditory prosthesis subjects. J. Acoust. Soc. 82:106-115.

Tyler RS, Preece JP, Tye-Murray N. (1986) The Iowa Phoneme and Sentence Tests (a laser video disc with consonant, vowel, and sentence tests), Department of Otolaryngology – Head and Neck Surgery, The University of Iowa, Iowa City, IA.

van den Honert, C. and Stypulkowski, PH. (1987a) Single fiber mapping of spatial excitation patterns in the electrically stimulated auditory nerve. Hear. Res., 29:195-206.

van den Honert, C. and Stypulkowski, PH. (1987b). Temporal response patterns of single auditory nerve fibers elicited by periodic electrical stimuli. Hear. Res., 29:195-206.

Van Tassell, DJ, Soli, SD, Kirby, VM, Widin, GP. (1987) Speech waveform envelope cues of consonant recognition. J. Acoust. Soc. Am. 82:1152-1161.

Van Tassel, DJ, Greeenfield, DG, Logemann, JJ, Nelson, DA. (1992) Temporal cues for consonant recognition: Training, talker generalization, and use in evaluation of auditory prostheses. J. Acoust. Soc. Am. 92:1247-1257.

Viemeister, N.F. (1979) Temporal modulation transfer functions based upon modulation thresholds. J. Acoust. Soc. Am. 82:1152-1161.

Viemeister, NF, Plack, CJ. (1993) Time analysis. In: *Human Psychophysics,* Yost, WA, Popper, AN, Fay, RR. pp 116-154. Springer, New York.

Vollmer, M, R.L. Snyder et al (1999) Effects of chronic intracochlear electrical stimulation and long term deafness on temporal response properties in the IC of neonatally deafened cat. J. Neurophysiol. . 82: 2883-2902.

Wardrop, P, Rebscher, SJ, Roland, JT, Leake, PA. (2001) A temporal bone study of insertion trauma and intracochlear position of auditory prosthesis electrodes. I: comparison of Cochlear banded and Cochlear Contour electrodes. (in press).

Wardrop, PJ, Rebscher, SJ, Leake, PA. 2000. Evaluation of Newer Auditory prosthesis Electrodes. 5th European Symposium on Peadiatric Auditory prosthesisation, Antwerp Belgium.

Wardrop, P, Rebscher SJ, Roland, JT, Leake, PA. (2002) Temporal Bone Study of Insertion Trauma and Intracochlear Position of Auditory prosthesis Electrodes. I: Comparison of Cochlear Banded and Cochlear Contour™ Electrodes. (In preparation, see Appendix XX)

Wardrop, P, Rebscher SJ, Luxford, W, Leake, PA. (2002a) A Temporal Bone Study of Insertion Trauma and Intracochlear Position of Auditory prosthesis Electrodes. II: Comparison of Advanced Bionics *Spiral Clarion*™ and *HiFocus*™ Electrodes. (In preparation, see Appendix XX)

Whinney , DJ, Rebscher, SJ, Leake, PA. (2002) Does the use of a lubricant to facilitate auditory prosthesis electrode insertion influence final insertion depth and insertion trauma? A temporal bone study. (In preparation, see Appendix XX)

Wier CC, Jesteadt W, Green DM (1977) Frequency discrimination as a function of frequency and sensation level. J. Acoust. Soc. Am. 61:178-184

Wilson, BS, Finley, CC, Lawson, DT, Zerbi, M. (1997) Temporal representations with auditory prostheses. Am. J. Otol. 18:S30-S34

Wilson, BS. (2000) Strategies for representing speech information with auditory prostheses. In: Auditory prostheses: Principles & Practices. Niparko, JK, Mellon, NK, Robbins, AM, Tucci, DL, Wilson, BS, eds. Lippincott Williams & Wilkins. Philadelphia.

Yang, L, Pollak, GG, Resler, C. (1992) GABAergic circuits sharpen tuning curves and modify response properties in the mustache bat inferior colliculus J. Neurophysiol. 68:1760-1774.

Young ED, Brownell WE. (1976) Responses to tones and noise of single cells in dorsal cochlear nucleus of unanesthetized cats. J Neurophysiol 39: 282-300.

Zurita P, Villa AEP, Deribaupierre Y, Deribaupierre F, Rouiller EM. (1994) Changes of single unit activity in the cat's auditory thalamus and cortex associated to different anesthetic conditions. Neurosci Res 19: 303-316,

Zhang, Y; Suga, N. (2000) Modulation of responses and frequency tuning of thalamic and collicular neurons by cortical activation in mustached bats**.** J. Neurophysiology 84:325-33.

Work Planned for the Next Quarter

1) Analysis of data and completion of figures is planned for preparation of a manuscript describing our "long-deafened" experimental series. This work investigated the consequences of severe neural degeneration upon electrophysiological thresholds, dynamic range and the effects of chronic stimulation in this model of severe cochlear pathology.

2) Chronic stimulation will be completed and the final experiment conducted in the second of 3 animals in a new chronic series in which profound hearing losses are induced at 1 month of age using acute administration of kanamycin/ethacrynic acid, rather than the neonatal prolonged administration of neomycin used in most prior studies.

3) Work will continue on further development of software for multichannel recording experiments examining spatial selectivity of electrical stimulation in guinea pigs and cats using the 16 electrode Michigan probe.

4) Several members of the UCSF cochlear implant research group (Drs. Leake, Snyder, Moore, Beitel, and Vollmer) will attend the 2002 Midwinter Research Meeting of the Association for Research in Otolaryngology to present work conducted for this Contract.